frontiers in Oncology

ORIGINAL RESEARCH
published: 24 November 2021
doi: 10.3389/fonc.2021.779739

Hypoxia Regulates Endogenous Double-Stranded RNA Production *via* Reduced Mitochondrial DNA Transcription

Esther Arnaiz[1,2‡], Ana Miar[1,3‡], Antonio Gregorio Dias Junior[4†], Naveen Prasad[3], Ulrike Schulze[5], Dominic Waithe[5], James A. Nathan[2], Jan Rehwinkel[4] and Adrian L. Harris[1]*

[1] Department of Medical Oncology, Molecular Oncology Laboratories, Weatherall Institute of Molecular Medicine, John Radcliffe Hospital, University of Oxford, Oxford, United Kingdom, [2] Cambridge Institute for Therapeutic Immunology & Infectious Disease, Jeffrey Cheah Biomedical Centre, Cambridge, United Kingdom, [3] Department of Oncology, Old Road Campus Research Building, University of Oxford, Oxford, United Kingdom, [4] Medical Research Council Human Immunology Unit, Weatherall Institute of Molecular Medicine, Radcliffe Department of Medicine, University of Oxford, Oxford, United Kingdom, [5] Radcliffe Department of Medicine, Weatherall Institute of Molecular Medicine, John Radcliffe Hospital, University of Oxford, Oxford, United Kingdom

Hypoxia is a common phenomenon in solid tumours strongly linked to the hallmarks of cancer. Hypoxia promotes local immunosuppression and downregulates type I interferon (IFN) expression and signalling, which contribute to the success of many cancer therapies. Double-stranded RNA (dsRNA), transiently generated during mitochondrial transcription, endogenously activates the type I IFN pathway. We report the effects of hypoxia on the generation of mitochondrial dsRNA (mtdsRNA) in breast cancer. We found a significant decrease in dsRNA production in different cell lines under hypoxia. This effect was HIF1α/2α-independent. mtdsRNA was responsible for induction of type I IFN and significantly decreased after hypoxia. Mitochondrially encoded gene expression was downregulated and mtdsRNA bound by the dsRNA-specific J2 antibody was decreased during hypoxia. These findings reveal a new mechanism of hypoxia-induced immunosuppression that could be targeted by hypoxia-activated therapies.

Keywords: hypoxia, IFN, dsRNA, mitochondria, cancer

OPEN ACCESS

Edited by:
Jonathan Pol, Institut National de la Santé et de la Recherche Médicale (INSERM), France

Reviewed by:
Keiko Kan-o, Kyushu University, Japan
Shona Mookerjee, Touro University California, United States

****Correspondence:***
Adrian L. Harris
adrian.harris@oncology.ox.ac.uk

†Present address:
Antonio Gregorio Dias Junior, Division of Infectious Diseases and Vaccinology, School of Public Health, University of California, Berkeley, Berkeley, CA, United States

‡These authors have contributed equally to this work and share first authorship

Specialty section:
This article was submitted to Cancer Immunity and Immunotherapy, a section of the journal Frontiers in Oncology

Received: *19 September 2021*
Accepted: *05 November 2021*
Published: *24 November 2021*

Citation:
Arnaiz E, Miar A, Dias Junior AG, Prasad N, Schulze U, Waithe D, Nathan JA, Rehwinkel J and Harris AL (2021) Hypoxia Regulates Endogenous Double-Stranded RNA Production via Reduced Mitochondrial DNA Transcription. Front. Oncol. 11:779739. doi: 10.3389/fonc.2021.779739

INTRODUCTION

Type I interferons (IFNs) include 13 IFNα subtypes, IFNβ, IFNε, IFNκ and IFNω, and type II and type III IFNs include IFNγ and IFNλ1-4, respectively. All IFNs are involved in the innate immune response against pathogenic infection. Type I and III IFNs are induced when specific microbial products, known as pathogen-associated molecular patterns (PAMPs), are detected by pattern-

Abbreviations: Interferon (IFN), IFN-stimulated genes (ISGs), double-stranded RNA (dsRNA), mitochondrial dsRNA (mtdsRNA), double-stranded DNA (dsDNA), mitochondrial DNA (mtDNA), mitochondrial RNA (mtRNA), mitochondrial ribosomal proteins (MRPs).

recognition receptors (PRRs) (1, 2). PRRs include Toll-like receptors (TLRs), some of which are specialised to survey the endosomal compartment for nucleic acids. In the cytosol, retinoic acid-inducible gene I (RIG-I) and melanoma differentiation-associated gene 5 (MDA5) detect unusual RNA molecules, as well as protein kinase R (PKR), which is also present in the mitochondria (3), while cyclic GMP-AMP (cGAMP) synthase (cGAS) is the major cytosolic double-stranded DNA (dsDNA) sensor and activates stimulator of interferon genes (STING).

Recognition of viral RNA by RIG-I and MDA5 induces protein conformational changes, which allows interaction with the shared adaptor mitochondrial antiviral-signaling protein (MAVS) that then triggers phosphorylation of interferon-regulatory factor 3 (IRF3) and IRF7. These transcription factors induce the expression of type I and III IFNs, chemokines, inflammatory cytokines and other genes (4). All type I IFNs bind a common receptor formed by IFNAR1 and IFNAR2, which through tyrosine kinase 2 (TYK2) and Janus kinase 1 (JAK1) recruits and phosphorylates signal transducer and activator of transcription (STAT) proteins (5). The canonical IFNAR signalling cascade involves STAT1 and STAT2, which form a ternary complex called interferon-stimulated gene factor 3 (ISGF3) with interferon-regulatory factor 9 (IRF9). ISGF3 translocates to the nucleus where it activates the transcription of IFN-stimulated genes (ISGs) (2). PKR is an ISG that binds to dsRNA and phosphorylates the α subunit of the eukaryotic initiation factor 2 (eIF2α) leading to general protein synthesis inhibition in order to restore cellular homeostasis upon viral infection (6). Moreover, it has been described that PKR interacts with several members of the TRAF family involved in MAVS signalling, such as TRAF2 and TRAF6 (7), and further contributing to the IFN response, it can also mediate phosphorylation of STAT1 (6).

Interestingly, type I IFNs can be produced in the absence of infection and are involved in the success of many anticancer treatments such as radiotherapy, chemotherapy, immunotherapy and oncolytic viruses (8), promoting direct (tumour cell growth inhibition) and indirect (antitumour immune response) effects (9).

Hypoxia generates an immunosuppressive microenvironment within the tumour by impeding the homing of immune effector cells and blocking their activity (10). Additionally, tumours contain more immunosuppressive cells, such as myeloid-derived suppressor cells (MDSCs), tumour-associated macrophages (TAMs) and T-regulatory (Treg) cells, in hypoxic regions (10, 11).

Lactate, generated during the metabolic switch to glycolysis under hypoxia, acts as a 'signalling molecule' and attenuates the cytotoxic activity of cytotoxic T cells (CTLs) (12) and natural killer (NK) cells (13), helps recruit myeloid-derived suppressor cells (MDSCs) to the tumour (13), and inhibits type I IFN induction *via* MAVS (14).

Mitochondrial DNA (mtDNA) is a closed-circular, dsDNA molecule of about 16.6kb and contains 37 genes coding for two rRNAs, 22 tRNAs and 13 polypeptides (15). Its complementary DNA strands are called H (heavy) and L (light). The L strand is the main coding strand containing the sense sequence of rRNAs and most of the tRNAs and mRNAs. Therefore, these RNAs are transcribed from and hybridize with the H strand (16). Mitochondria generate a number of damage-associated molecular patterns (DAMPs) including ATP, succinate, cardiolipin, N-formylpeptides, mitochondrial transcription factor A (TFAM), cytochrome-c, mtDNA and mitochondrial RNA (mtRNA) (17). Extracellular mtDNA binds to TRL9 (18) whereas cytosolic mtDNA is recognised by inflammasomes (19) and cGAS (20). More recently, mtRNA was described to be a potent DAMP *via* recognition of a specific segment of the mitochondrial single-stranded rRNA by TLR8 (21). In addition, dsRNA originating from convergent mtDNA transcription triggers an MDA5-dependent type I IFN response when released to the cytoplasm (22).

Previously, we showed that the type I IFN responses induced by exogenous dsRNA are downregulated under hypoxia in cell lines from different solid tumors *via* transcriptional repression after changes in chromatin conformation (23). Here, we investigated the role of hypoxia in the regulation of endogenous dsRNA formation and function. We have shown that hypoxia decreases the formation of mtdsRNA, probably by reducing the mitochondrial transcription rate, and lowers the endogenous activation of the type I IFN pathway. This effect is HIF1α/2α independent and occurs in different cancer cell lines as well as non-transformed cell lines. Moreover, different tissues have different immunostimulatory potential.

MATERIALS AND METHODS

Biological Resources

Human total RNA from different tissues used in this study was purchased to Takara Bio/Clontech (Shiga, Japan).

MCF7, T47D, BT474, MDA-MB-231, MDA-MB-453, MDA-MB-468, RCC4, 786-0, U2OS mTUNE, and human fibroblasts were cultured in DMEM low glucose medium (1g/L; Thermo Fisher Scientific, Waltham, Massachusetts) supplemented with 10% FBS no longer than 20 passages. HUVEC cells were purchased from Lonza (Basilea, Switzerland) and grown in EGM2 medium for maximum 7 passages. They were all mycoplasma tested every 3 months and authenticated during the course of this project. Cells were subjected to 1% or 0.1% hypoxia for the periods specified in each experiment using an $InVivO_2$ chamber (Baker, Sandford, Maine).

U2OS mTUNE glioblastoma cell lines were kindly donated by Dr Christian Frezza. Three isogenic cell lines with different levels of heteroplasmy of mutated mtDNA were used: M7, M45 and M80 (24).

143B and 143B Rho Zero (Rho Zero) cells were a gift of Dr Karl Morten. Rho Zero cells were generated by treating 143B cells (TK1 deficient) with 10μM 2',3'-dideoxycytidine (ddC) for 10 days. Both cell lines were grown in high glucose DMEM (Gibco, Carlsbad, California) supplemented with 10% FBS. Rho Zero cell culture media was additionally

supplemented with 50μg/mL uridine (A15227.06, Alfa Aesar, Haverhill, Massachusetts).

Drug Treatment

MCF7 cells were cultured in normoxia or 0.1% hypoxia and treated for 48h with the following mitochondria-targeting drugs: 5μM Vps34 inhibitor SAR405 (16979, Cayman Chemical, Ann Harbor, Michigan), 200μM chloramphenicol (C0378, Sigma-Aldrich, St Louis, Missouri), 100nM mubritinib (S-2216, Selleckchem, Houston, Texas), 5μM ABT-737 (sc-207242, Santa Cruz Biotechnology, Dallas, Texas), 2mM metformin (D150959, Sigma-Aldrich), 5μM gamitrinib-triphenylphosphonium (G-TPP, HY-102007, MedChemExpress, Monmouth Junction, New Jersey), 1μM/10μM IMT1 (HY-134539, MedChemExpress) or 1μM NBS-037 (Novintum Bioscience Ltd., London, England) (25).

siRNA Transfection

BNIP3 siRNA transfection (**Supplementary Table 1**) was performed in Optimem reduced serum medium at a final concentration of 5nM, the following day cells were exposed to 0.1% hypoxia for 48h. siRNA control was done in parallel and the following day was subjected to normoxia or 0.1% hypoxia for 48h. Oligofectamine (12252-011, Thermo Fisher Scientific) was used following the manufacturer's instructions.

Western Blot

Whole cell lysates were prepared with RIPA buffer (R0278, Sigma-Aldrich) containing protease (cOmplete, 11697498001, Sigma-Aldrich) and phosphatase (phosSTOP, 4906845001, Sigma-Aldrich) inhibitors. Samples were subjected to SDS-PAGE and transferred onto PVDF membranes (IPVH00010, Millipore, Burlington, Massachusetts), after blocking, membranes were incubated overnight with primary antibodies (**Supplementary Table 2**) at 4°C. They were later washed and incubated with HRP-anti-mouse/rabbit secondary antibodies (Gibco). Development was performed with Amersham ECL Prime Western Blotting Detection Reagent (GERPN2232, GE Healthcare Life Sciences, Chicago, Illinois) using ImageQuant™ LAS 4000. Stripping with Restore PLUS Western Blot Stripping Buffer (46430, Invitrogen, Carlsbad, California) was performed to blot different antibodies in the same membrane.

RT-qPCR

RNA was extracted using the Tri-Reagent protocol (T9424, Sigma-Aldrich) and 1μg was reverse transcribed with the High Capacity cDNA reverse transcription kit (44368813, Thermo Fisher Scientific) using random hexamer primers. The PCR reaction containing SensiMix™ SYBR Green® No-ROX Kit (QT650-20, Bioline, London, UK) was run on a 7900 Real time PCR System (Applied Biosystems, Foster City, California) with standard cycling conditions: 10 minutes 95°C, and 40 cycles of 15 seconds 95°C followed by 1 minute 60°C. Gene expression was analysed with the Ct method using *HPRT1* expression for normalization. The primers used are listed in **Supplementary Table 3**.

IFNβ Promoter Reporter Assay

HEK293T-P125 reporter cells (stably expressing the *IFNβ* promoter-Luciferase region (26)) were used to detect specifically immunostimulatory RNAs as they do not express cGAS and the expression of STING is very low. $4x10^4$ cells per well were seeded in 96-well plates. Next day, cells were pre-treated with 30U/mL of IFN-A/D (I4401, Sigma-Aldrich), and after 24h of incubation fresh medium was added and cells were transfected with 100ng of total RNAs from cell cultures or human tissues using Lipofectamine 2000® (11668-019, Thermo Fisher Scientific). As positive controls, 1ng of IVT-RNA or V-EMCV-RNA was used (26). 24h post-transfection, cells were lysed and measured using OneGlo luciferase assay (E6120, Promega, Madison, Wisconsin) in a FluorOPTIMA luminometer.

Immunofluorescence for dsRNA or PKR

Cells were plated on coverslips (VWR Collection, Radnor, Pennsylvania) and exposed to 0.1% O_2 hypoxia for 48h. Prior to fixation, mitochondria were stained for 1h with 200nM MitoTracker Deep Red (M22426, Thermo Fisher Scientific). After, cells were washed and fixed with 4% (v/v) paraformaldehyde (PFA) for 8 min at room temperature (RT). Then, cells were washed and permeabilized with 0.1% Triton X-100 for 20 min at RT. PFA was neutralized with 0.1M glycine for 10 min at RT. After washing three times, cells were incubated for 60 min with blocking solution [PBS containing 1% (w/v) BSA and 10% (v/v) normal goat serum (ab7481, Abcam, Cambridge, UK)]. Cells were incubated overnight at 4°C in a humidified chamber with J2 primary antibody (10010200, Scicons, Szirák, Hungary) at 1:200 or PKR (sc-6282, Insight Biotechnology Ltd, Wembley, UK) at 1:50, and rhodamine phalloidin (R415, Invitrogen) at 1:40 in block solution. Cells were washed three times and incubated with goat anti-mouse IgG Alexa Fluor 488 (R37120, Invitrogen) secondary antibody at 1:500 and Hoechst 33342 (H3570, Invitrogen) at 1:1000 concentration in block solution for 1h at RT. After washing three times with PBS, coverslips were mounted with Vectashield® Mounting Medium (H-1000, Vector Labs, Burlingame, California) and sealed with nail polish.

Immunofluorescence dsRNA Image Analysis

Slides were imaged in a Zeiss 880 Inverted confocal microscope (Zeiss) using a 63x Plan-Apochromat objective. Laser properties, acquisition mode and detectors were manually adjusted for each experiment. Fiji Image J software was used for image analysis, using specific macros created by Dr Ulrike Schulze and Dr Dominic Waithe. A minimum of 35 cells per condition were analysed.

Live Cell Immunofluorescence

$2x10^4$ MCF7 cells were seeded in 24-well glass-bottom SensoPlate™ (662892, Greiner) for 48h. 1h prior to imaging, media was removed and replaced with complete DMEM containing 50nM LysoTracker™ Red DND-99 (L7528, Invitrogen™) and 100nM MitoTracker™ Green FM (M7514,

Invitrogen™). Then, media was removed and replaced with fresh media. Living cells were imaged in a Zeiss 880 Inverted confocal microscope (Zeiss) using a ZEN fluorescence microscopy system (Zeiss) and a 63x Plan-Apochromat objective. Laser properties, acquisition mode and detectors were manually adjusted for each experiment.

Mitochondria Extraction

Mitochondria were isolated from MCF7 cells seeded in normoxia or 0.1% hypoxia for 48h using Mitochondria Isolation Kit for Cultured Cells (89874, Thermo Fisher Scientific) and following manufacturer's instructions. Mitochondrial RNA was extracted using Tri Reagent, following the protocol previously explained. In step 8 of manufacturer's instructions, the cytosolic fraction was kept and 200uL were used to extract RNA.

Immunoprecipitation of dsRNA

Protein G Dynabeads (10004D, Invitrogen) were washed and resuspended in NET-2 buffer. 5μg of J2 antibody or mouse IgG2 (400201, BioLegends, San Diego, California) were bound to 100μL of beads for 1h at RT on a thermoshaker. Conjugated beads were washed three times with NET-2 Buffer. 80–90% confluent MCF7 cells from 10cm^2 plate (×2) were washed with 10mL of cold PBS. Cells were scraped and transferred to a falcon and spun at 500*g* at 4°C, 5 min. Cell pellet from one 10cm^2 plate was lysed in 1mL of NP-40 lysis buffer and transferred to a tube and incubated on ice for 5 min. Following centrifugation at 17,000*g* at 4°C for 5 min, supernatant was carefully transferred to a new tube. Total RNA was harvested from 10% input lysate using Tri Reagent. For immunoprecipitation, lysate was supplemented with 10 units of RNase free TurboDNase (AM2238, Thermo Fisher Scientific) at 10mM $MgCl_2$ per 1mL of mix. 100μL of J2-Dynabeads was added to 1mL of above lysate and left for 1–2h at 4°C. Following magnetic separation, beads were washed twice with 1mL of high salt washing buffer (HSWB). Beads were transferred to a new tube with NET-2 buffer and washed twice with the same buffer. J2-bound dsRNA was extracted with Tri Reagent. The RNA samples were sent for sequencing. NET-2 buffer (50mM Tris-Cl, pH 7.4, 150mM NaCl, 1mM $MgCl_2$, 0.5% NP-40), NP-40 lysis buffer (50mM Tris-Cl pH 7.4, 150mM NaCl, 5mM EDTA, 0.5% NP-40), high salt wash buffer (50mM Tris-Cl pH 7.4, 1M NaCl, 1mM EDTA, 1% NP-40, 0.5% DOC, 0.1% SDS).

RNA-Sequencing and Data Analysis

Libraries for paired end sequencing were prepared using standard Illumina protocol and sequencing was performed using Illumina NovoSeq 6000 sequencer at Wellcome Centre for Human Genetics. Raw reads were processed using FASTQC and Cutadapt and aligned to the genome using STAR. Normalised counts of nuclear encoded genes involved in mitochondrial function and mitochondrial encoded genes were used for generation of heatmaps. In order to estimate the proportion of counts that map to mitochondrial and non-mitochondrial genes; transcript per million (TPM) normalized value of transcripts encoded by mitochondrial and non mitochondrial genome in different replicates was calculated. Proportion of TPM counts in mitochondrial or non-mitochondrial fractions was calculated by dividing the sum of TPM counts in the fraction by total TPM counts.

Statistical Analysis

GraphPad Prism 8.0 statistical analysis software (GraphPad Software) was used. If not otherwise specified, all the experiments were performed in 3 biological triplicates. ANOVA or ANOVA on ranks was normally used to study one variable in more than 2 groups depending on if they follow a normal distribution or not respectively. When two means were compared, t-test was performed if samples followed a normal distribution or Mann-Whitney if there was not a normal distribution. When analysing the βluence of two different independent variables on one dependent variable, 2-way ANOVA was applied. In the graphs, the error bars depict the standard error of the mean (SEM).

RESULTS

Hypoxia Prevents the Accumulation of Immunostimulatory RNAs

Given the immuno-suppressive role of hypoxia, we tested whether cancer cell lines cultured in normoxia or hypoxia contain different amounts of immunostimulatory RNA. We extracted total RNA from the breast cancer cell line MCF7 cultured for 48 hours in normoxia or in 1% or 0.1% hypoxia. We then transfected this RNA into an *IFNβ* promoter reporter cell line (26). RNA from cells grown in normoxia induced expression of the reporter, indicative of the presence of immunostimulatory RNA (**Figure 1A**). To determine the sensor for this endogenous RNA, we tested the response in reporter cells lacking MDA5, RIG-I or MAVS. This analysis showed that total RNA from MCF7 cells induced an MDA5-MAVS-dependent response (**Figure 1A**). Interestingly, RNA from hypoxic cells (hypoxic RNA) had a significantly reduced capacity to induce activation of the *IFNβ* promoter reporter compared with RNA from normoxic cells (normoxic RNA; **Figure 1A**). Moreover, much like the response to normoxic RNA, residual reporter induction after hypoxic RNA transfection was MDA5-MAVS-dependent and RIG-I-independent (**Figure 1A**).

As 0.1% hypoxia had a greater effect than 1% hypoxia (**Figure 1A**), subsequent experiments were performed under 0.1% hypoxic conditions. A time course in hypoxia for 4h, 8h, 16h, 24h and 48h showed that 4h in hypoxia was enough to lower *IFNβ* promoter stimulation and it was maintained up till 48h (**Figure 1B** left panel). The time course for recovery after reoxygenation following 48h hypoxia was evaluated at 15min, 30min, 1h, 2h, 4h, 8h, 16h and 24h. Reoxygenation caused a gradual recovery of *IFNβ* promoter stimulation reaching normoxic basal levels at 24h (**Figure 1B** right panel).

A panel of breast cancer cell lines with different receptor status were used to rule out a cell line dependent effect of hypoxia in MCF7 cells. Hypoxic RNA was much less effective than

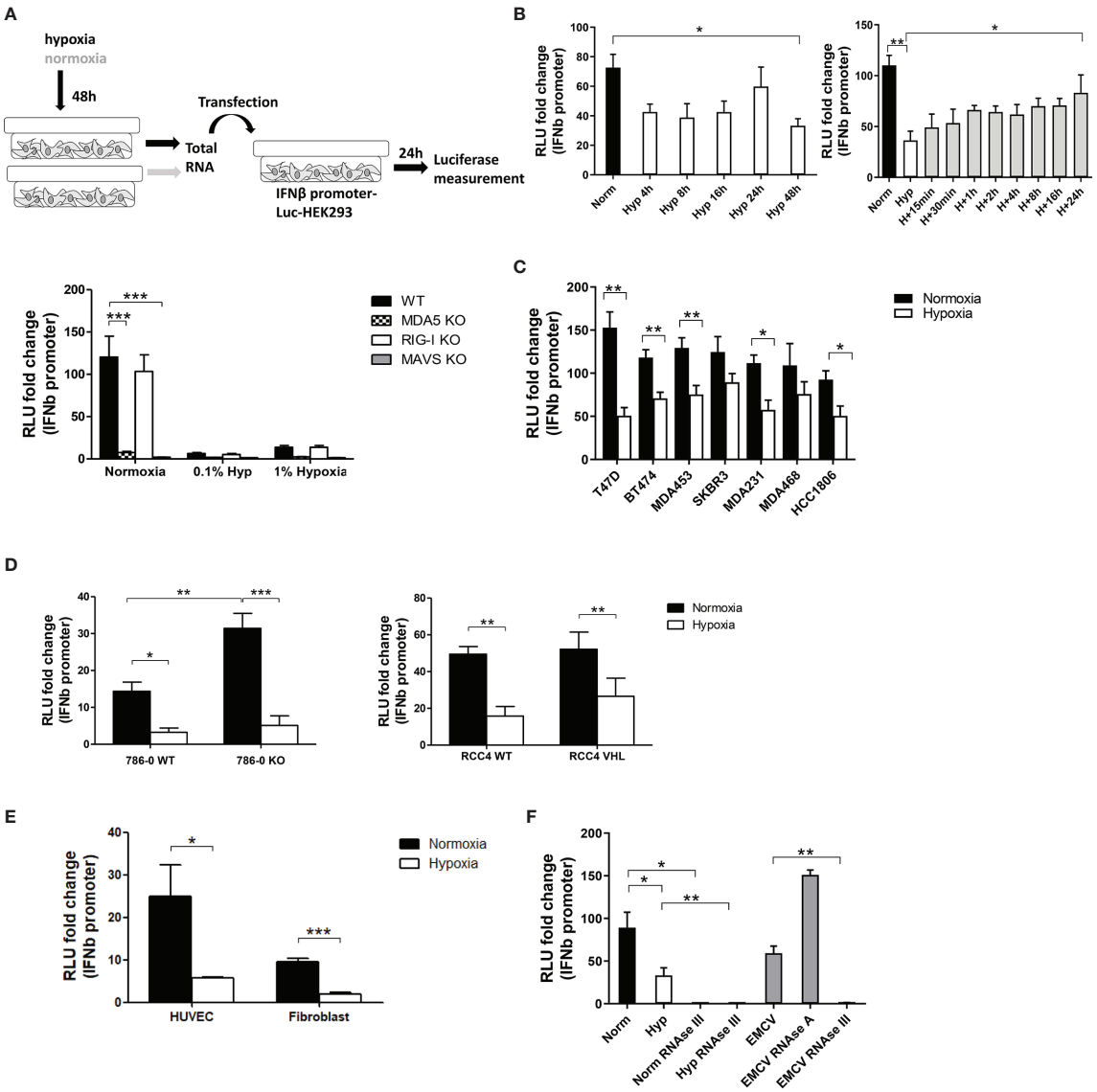

FIGURE 1 | Hypoxia decreased *IFNβ* promoter stimulation. **(A)** An outline of the experiment is shown (top, please see text for detail). *IFNβ* promoter reporter cells of the indicated genotypes were transfected with total RNA extracted from MCF7 cells exposed for 48h to normoxia, 1% hypoxia and 0.1% hypoxia. 24h after transfection, reporter cells were lysed and firefly luciferase activity was determined (bar charts; RLU, relative light units). Data from control cells treated with transfection reagent only were used to calculate RLU fold changes after RNA transfection (n=10). **(B)** *IFNβ* promoter stimulation time course using RNA from MCF7 cells exposed to normoxia or 0.1% hypoxia for 4h, 8h, 16h, 24h and 48h (left panel, n=3), and reoxygenation for 15min, 30min, 1h, 2h, 4h, 8h, 16h and 24h after 48h in 0.1% hypoxia (right panel, n=3). **(C)** *IFNβ* promoter stimulation using RNA from a panel of breast cancer cell lines exposed to normoxia or 0.1% hypoxia for 48h. **(D)** *IFNβ* promoter stimulation using RNA from 786-0 WT or 786-0 HIF2α KO cells (786-0 KO, left panel, n=3), and RCC4 EV or RCC4 VHL (right panel, n=3) exposed to normoxia or 0.1% hypoxia for 48h. **(E)** *IFNβ* promoter stimulation using RNA from non cancerous cell lines exposed to normoxia or 0.1% hypoxia for 48h (n=3). **(F)** *IFNβ* promoter stimulation using RNA from MCF7 cells treated with RNAse A or RNAse III, and EMCV dsRNA as positive control (n=3). Number of replicates indicate biological replicates and data is shown as mean ± SEM. *p < 0.05, **p < 0.01, ***p < 0.001.

normoxic RNA in stimulating *IFNβ* promoter in all cell lines (**Figure 1C**).

Hypoxic Reduction of dsRNA Formation Is HIF1α/2α Independent

Normoxic and hypoxic RNA from 786-0 WT (HIF1α deficient and HIF2α upregulated due to *VHL* mutation) and 786-0 HIF2α KO (hereafter 786-0 KO, HIF1α and HIF2α deficient), and RCC4 WT (*VHL* mutation leading to HIF1α and HIF2α constitutive overexpression) and RCC4 VHL (*VHL* restored causing HIF1α and HIF2α downregulation) was tested. In both cell lines and all genotypes, hypoxic RNA triggered significantly lower *IFNβ* promoter stimulation (**Figure 1D**), highlighting the HIF-independent effect. However, 786-0 KO

cells showed higher *IFNβ* promoter activation under normoxia compared to 786-0 WT, suggesting an effect of HIF2α in suppressing IFNβ induction, although minimal compared to the effect of hypoxia.

We also tested normal endothelial cells (HUVECS) and fibroblasts. Again, hypoxic RNA significantly reduced the activation of *IFNβ* promoter (**Figure 1E**) pointing to a general effect of hypoxia independently of cancer.

To analyse which RNA species from the total RNA were responsible for the *IFNβ* promoter induction, normoxic and hypoxic RNA from MCF7 cells was treated with different RNAses and EMCV (*Encephalomyocarditis Virus*), containing only dsRNA, was used as positive control. RNAse III (specific for dsRNA) treatment completely abolished normoxic, hypoxic and EMCV RNA induced *IFNβ* promoter activity, whereas RNAse A (specific for single-stranded RNA, ssRNA) treatment did not affect the luciferase signal (**Figure 1F**), showing that endogenous dsRNAs are responsible for the *IFNβ* promoter activation rather than ssRNA.

Imaging of dsRNA Levels Downregulation Under Hypoxia

To visualise the downregulation of dsRNA levels in hypoxia, fluorescence microscopy was performed using the J2 antibody which is widely used to specifically detect dsRNA (22, 27). dsRNA staining was detected both inside (**Figure 2A** white arrow) and outside (**Figure 2A** blue arrow) mitochondria and although there was substantial variability of dsRNA intensity among individual cells, it was significantly lower in MCF7 hypoxic cells (**Figure 2A**). The downregulation was time-dependent and significant after 16h in hypoxia (**Figure 2B**). To confirm the HIF1α/HIF2α-independence observed in the *IFNβ* promoter assay, 786-0 WT and 786-0 KO cells were stained and both cell lines showed significantly lower dsRNA levels in hypoxia (**Figure 2C**).

As control for the antibody to dsRNA, MCF7 cells were treated with NBS-037, a drug inhibiting mitochondrial protein synthesis and secondarily mtRNA synthesis (25). NBS-037 treatment markedly decreased dsRNA levels (**Supplementary Figure 1**).

mtDNA and Effect Of Mutation Status on dsRNA in Hypoxia

It was recently shown that 99% of endogenous dsRNA originates during mtDNA transcription (22). Therefore, we tested cells lacking mtDNA (Rho Zero) and found significantly lower dsRNA staining in the Rho Zero cells than the parental 143B cell line (**Figure 3A**) and similar reduction in *IFNβ* promoter activation (**Figure 3B**). This strongly supports the specificity of the J2 antibody and the *IFNβ* promoter for dsRNA, and suggests that hypoxic downregulation of mtdsRNA relies on having functional mitochondria. Surprisingly, there was no difference between normoxia and hypoxia in the 143B parental cell line, either in the dsRNA staining or in the *IFNβ* promoter assay. This was the only cell line among all tested in which hypoxia did not downregulate the type I IFN pathway.

As hypoxia causes a shift to reductive carboxylation for glutamine utilisation by mitochondria (28), we considered that differences in metabolism in hypoxic mitochondria could contribute to mtdsRNA production. The mtDNA mutation m8993T>G affects ATP6, a key subunit of ATP synthase, leading to several serious diseases e.g. retinitis pigmentosa and fatal childhood maternally inherited Leigh's syndrome. Isogenic cell lines with different levels of heteroplasmy of the mtDNA mutation m8993T>G were generated. As the percentage of heteroplasmy for m8993T>G increased from 7 to 80% (U2OS mTUNE M7, M45, M80), oxygen consumption decreased and extracellular acidification increased, allowing intra-mitochondrial metabolism to be modified without manipulation (24). We aimed to see if this switch in glucose utilisation by mitochondria could affect mtRNA synthesis. The basal level of cytoplasmic dsRNA was similar in M7 and M45 (data not shown), but higher in M80 cells. However, hypoxia downregulated dsRNA levels in all mTUNE cell lines independently of the mutation level and metabolic profile (**Figure 3C**) and caused significantly lower *IFNβ* promoter activation (**Figure 3D**).

Moreover, it was previously reported that mtdsRNA accumulated when the degrading enzymes PNPT1 and SUV3 were inhibited, and downregulation of PNPT1 triggered the type I IFN pathway (22). However, neither PNPT1 nor SUV3 protein levels were affected by 0.1% hypoxia for 48h (**Figure 3E**).

PKR Preferentially Locates in the Nucleus Under Hypoxia

PKR, alongside RIG-I and MDA5, is a key member of the antiviral signaling hub activated by dsRNA molecules. It has been described to be located and activated in the mitochondria independently of PNPT1 deficiency (3). We therefore analysed the gene expression and protein levels of PKR in MCF7 cells and found that these were significantly downregulated in hypoxia both at mRNA (**Figure 4A** left panel) and protein (**Figure 4A** right panel) level. In addition, the downregulation was time-dependent (**Figure 4B**), starting to lower as soon as 4h of hypoxia exposure, but being significant after 16h, as previously seen for RIG-I and MDA5 (23). Furthermore, reoxygenation after hypoxia exposure recovered the expression levels of PKR (**Figure 4C**).

PKR locates in both the nucleus and the mitochondria, where it can interact with noncoding nuclear RNAs as well as mtRNA, respectively (3). Hypoxia increased the levels of PKR protein in the nucleus, staining specifically in the nucleolus, while decreasing the amount of PKR in the mitochondria. There were changes in mitochondria morphology as previously noted in hypoxia (29, 30) (**Figure 4D**).

Hypoxia Reduces mtDNA Transcription

We measured the expression of some mitochondrial encoded genes (*12S*, *ND3*, *ATP6* and *CYTB*) and also nuclear encoded genes involved in mtDNA transcription [*POLRMT* (mitochondrial RNA polymerase that catalyses mtDNA transcription), *TFAM* (which stabilizes mtDNA, regulates mtDNA transcription, and is required for efficient promoter recognition by POLRMT) and *TFB1M* (mitochondrial dimethyladenosine transferase 1 whose interaction with POLRMT and TFAM is required for mtDNA transcription)]. Both sets of genes were significantly downregulated in MCF7 cells cultured under 0.1% hypoxia (**Figure 5A**). Most of the

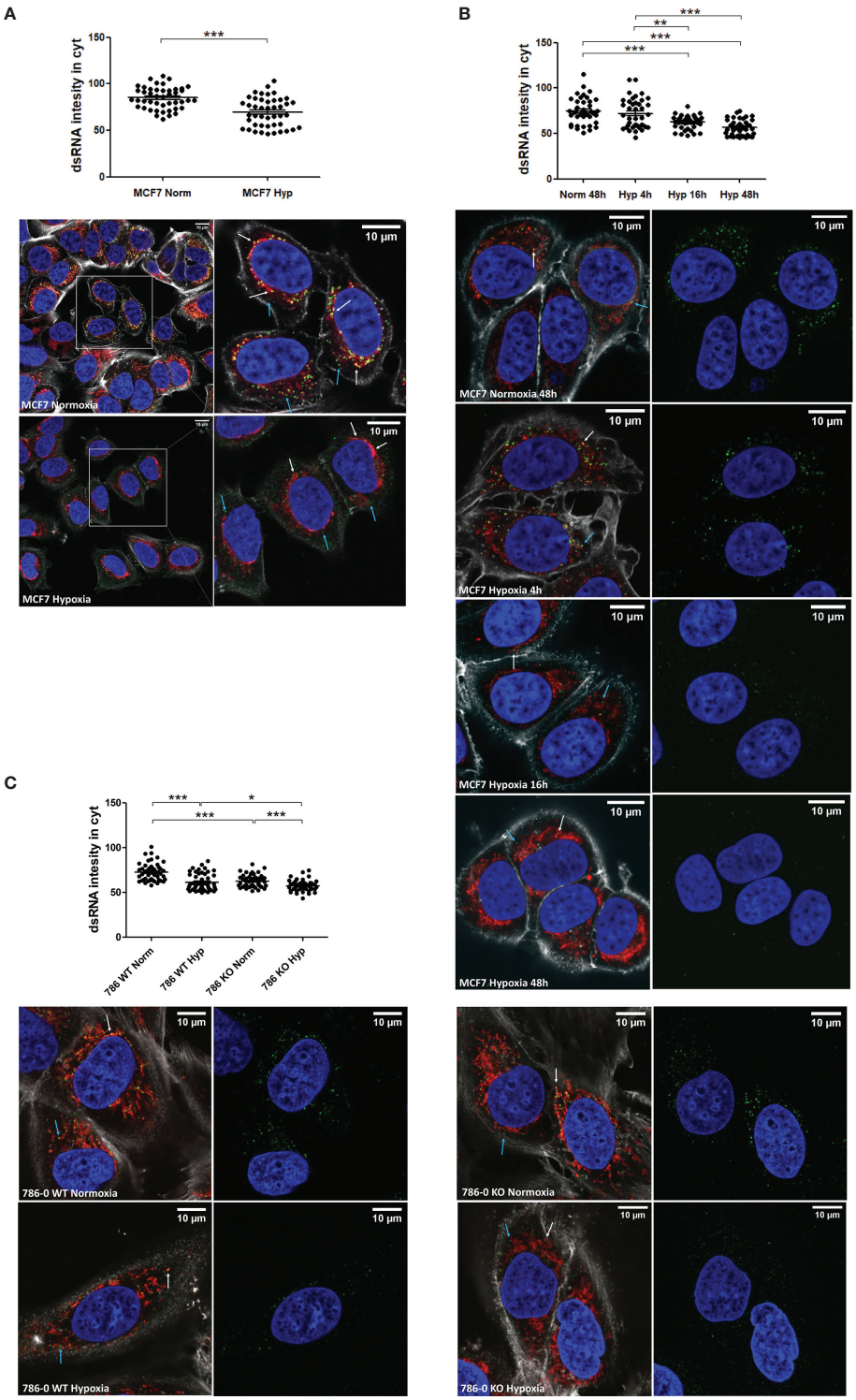

FIGURE 2 | dsRNA staining is significantly lower under hypoxia independently of HIF1α/2α expression. **(A)** dsRNA was stained using J2 antibody in MCF7 cells exposed to normoxia (n=45 cells) or 0.1% hypoxia (n=45 cells) for 48h from 3 independent replicates. **(B)** dsRNA was monitored during a time course of MCF7 cells in normoxia (n=40 cells), or exposed to 0.1% for 4h (n=40 cells), 16h (n=40 cells), and 48h (n=40 cells) from 3 independent replicates. **(C)** HIF1α/2α involvement was evaluated by staining dsRNA in 786-0 WT cells (786 WT, n=46 normoxic cells and n=46 hypoxic cells), and 786-0 HIF2α-KO cells (786 KO, n= 45 normoxic cells and n=45 hypoxic cells) from 3 independent replicates. Data is shown as mean ± SEM. *$p < 0.05$, **$p < 0.01$, ***$p < 0.001$. Green: J2 antibody staining, blue: DAPI, and red: MitoTracker staining. White arrow: dsRNA inside of mitochondria, blue arrow: dsRNA outside of mitochondria. Scale bars correspond to 10µm.

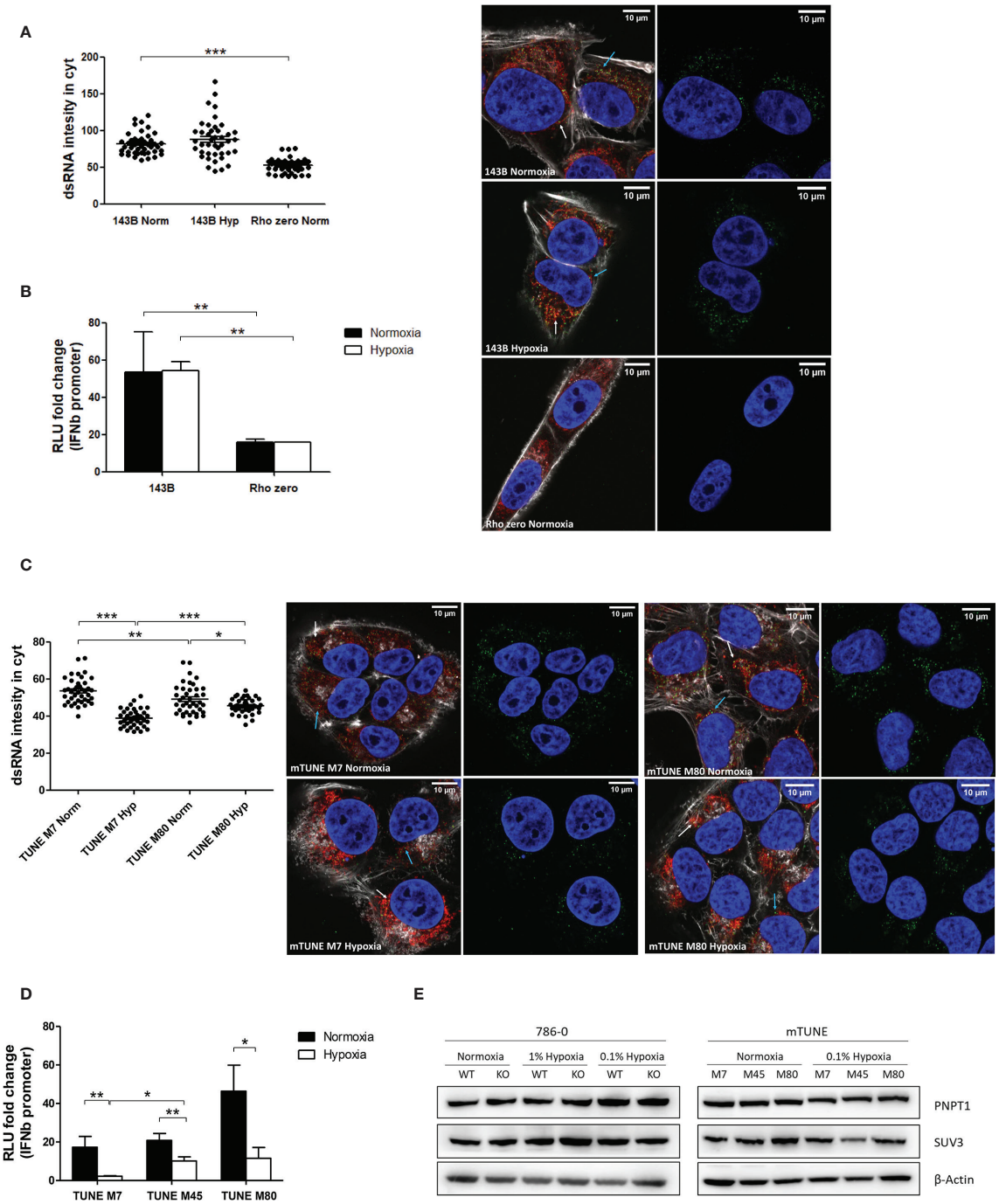

FIGURE 3 | Mitochondrial alterations did not affect dsRNA staining reduction under hypoxia. **(A)** Representative images showing dsRNA staining using J2 antibody in 143B WT cells in normoxia (n=44 cells) or 0.1% hypoxia (n=42 cells) for 48h and in 143B lacking mtDNA (Rho Zero) exposed to normoxia (n=40 cells) from 3 independent replicates. **(B)** *IFNβ* promoter stimulation was evaluated using RNA from 143B WT and Rho Zero cells cultured in normoxia and 0.1% hypoxia for 48h (n=3; RLU, relative light units). **(C)** Representative images showing dsRNA staining in U2OS isogenic lines harbouring 7% vs 80% of heteroplasmy for the mtDNA mutation m8993T>G (mTUNE M7 normoxia n=40 cells and 0.1% hypoxia n=40 cells, M80 normoxia n=40 cells and 0.1% hypoxia n=40 cells) from 3 independent replicates. **(D)** *IFNβ* promoter stimulation using RNA from mTUNE M7, M45 and M80 cells in normoxia and 0.1% hypoxia for 48h (n=3). **(E)** Western blot showing PNPT1 and SUV3 dsRNA degrading enzymes protein levels in normoxia and hypoxia (n=3). Number of replicates indicate biological replicates and data is shown as mean ± SEM. *p < 0.05, **p < 0.01, ***p < 0.001. Green: J2 antibody staining, blue: DAPI, and red: MitoTracker staining. White arrow: dsRNA inside of mitochondria, blue arrow: dsRNA outside of mitochondria. Scale bars correspond to 10μm.

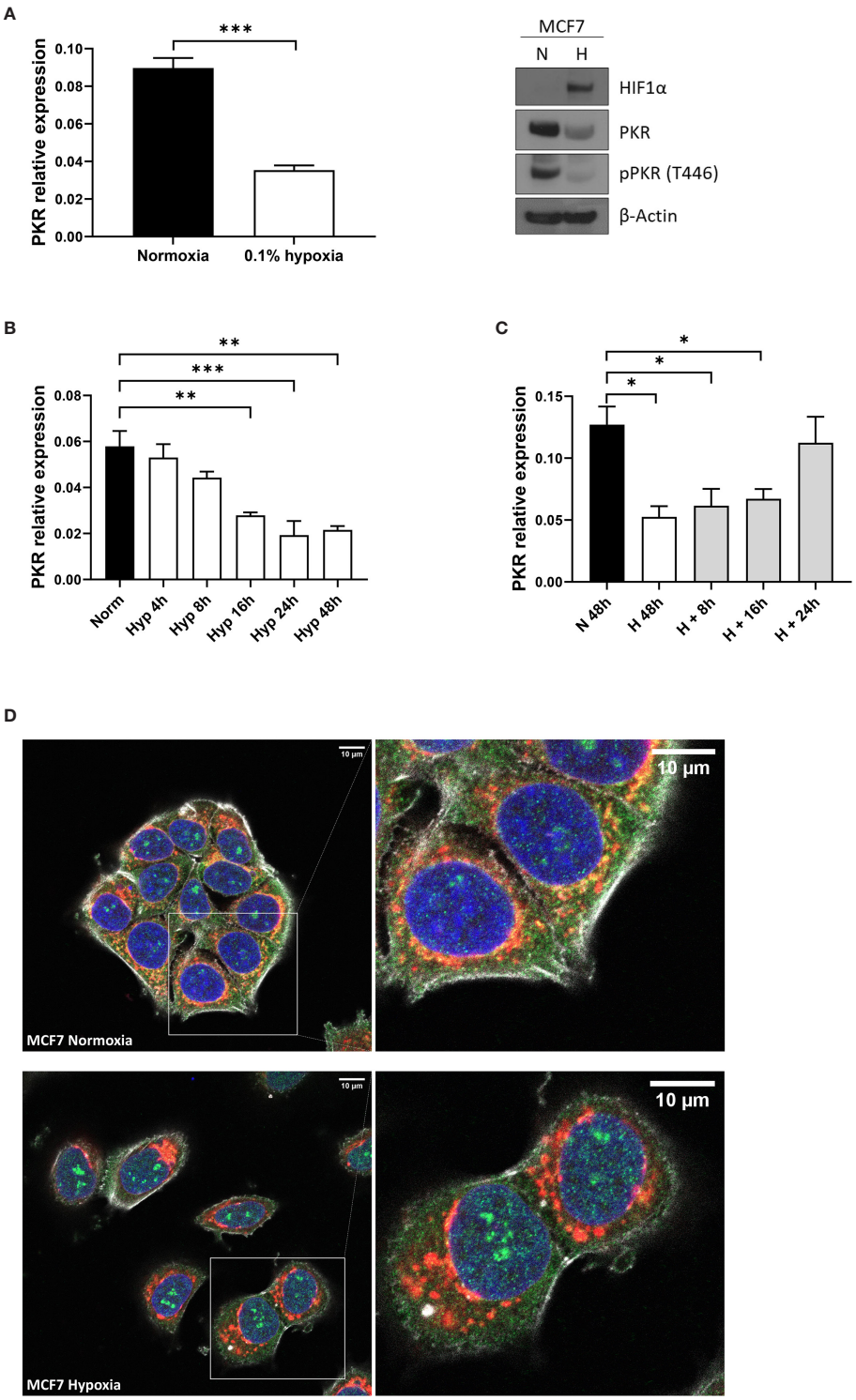

FIGURE 4 | PKR is downregulated in hypoxia. **(A)** PKR expression levels analysed by qPCR and western blot in MCF7 cells cultured in normoxia or 0.1% hypoxia for 48h (n=3). *PKR* mRNA expression was analysed in MCF7 cells cultured in normoxia or 0.1% hypoxia for 4h, 8h, 16h, 24h and 48h (n=3) **(B)** and in MCF7 cells cultured in 0.1% hypoxia for 48h and later reoxygenated for 8h, 16h and 24h (n=3) **(C)**. **(D)** PKR was stained using PKR antibody in MCF7 cells exposed to normoxia or 0.1% hypoxia for 48h from 3 independent replicates. Number of replicates indicate biological replicates and data is shown as mean ± SEM. *p < 0.05, **p < 0.01, ***p < 0.001. Green: PKR antibody staining, blue: DAPI and red: MitoTracker staining. Scale bars correspond to 10µm.

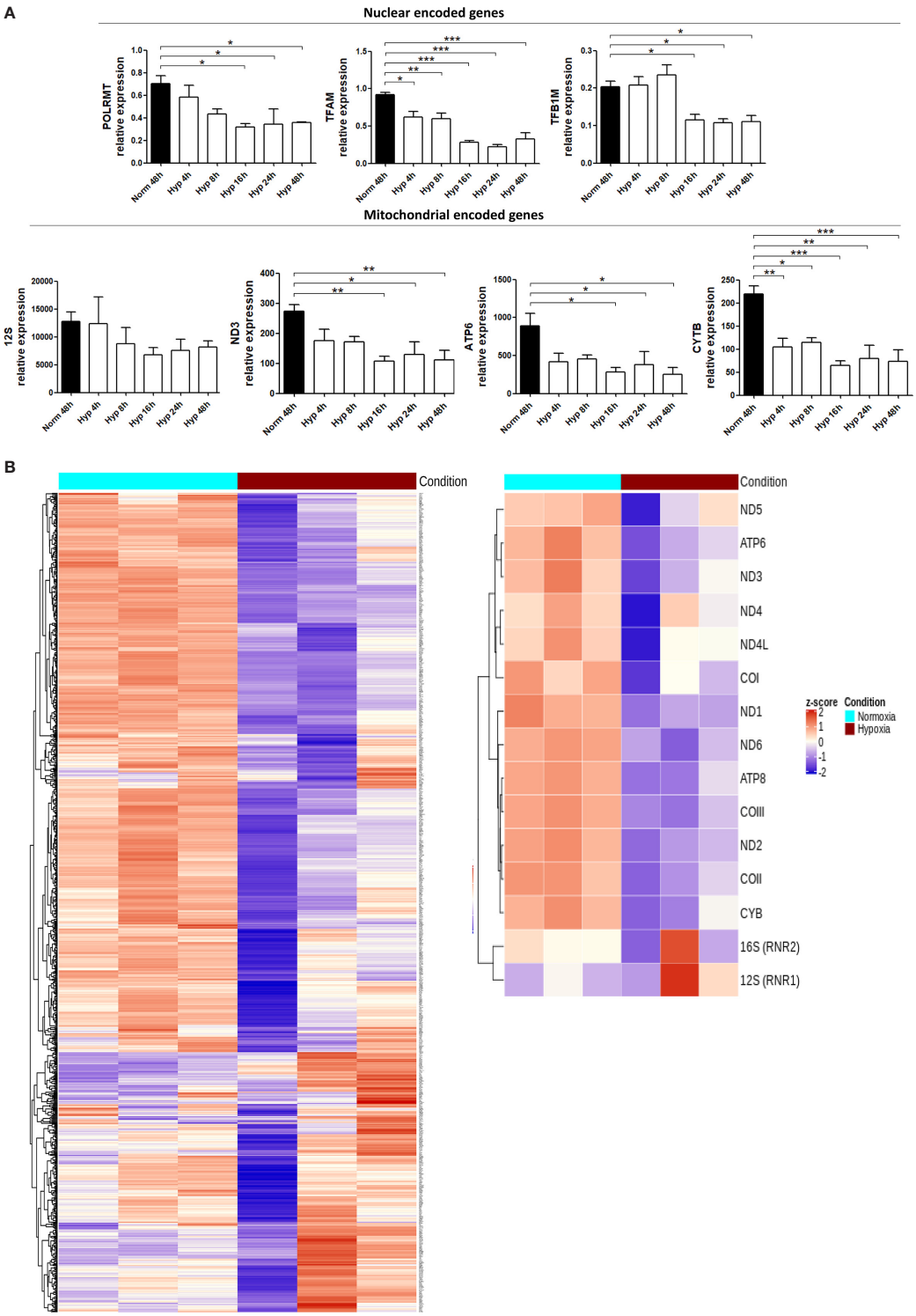

FIGURE 5 | Hypoxia downregulates the expression of mitochondrial genes. **(A)** RNA expression of mitochondrial encoded genes (*12S, ND3, ATP6, CYTB*) or nuclear encoded genes involved in mitochondrial function (*POLRMT, TFAM, TFB1M*) in MCF7 cells cultured in normoxia or 0.1% hypoxia for 4h, 8h, 16h, 24h and 48h was evaluated by qPCR (n=3). **(B)** Heatmap showing expression of mitochondrial encoded genes (right panel) or 1158 nuclear encoded genes involved in mitochondrial function (left panel, from MitoCarta 2.0) in MCF7 cells cultured in normoxia or 0.1% hypoxia for 48h (n=3) from RNAseq experiment described in Materials section. Number of replicates indicate biological replicates and data is shown as mean ± SEM. *p < 0.05, **p < 0.01, ***p < 0.001.

tested genes showed lower expression after only 4h under hypoxia (*POLRMT*, *TFAM*, *ND3*, *ATP6* and *CYTB*) but it was significant for all when cultured for 16h in hypoxia. These results were confirmed by the general downregulation observed in mitochondrial encoded genes and nuclear encoded genes involved in mitochondrial function [from MitoCarta 2.0 (31)] using RNA-seq data from MCF7 cells cultured in normoxia or 0.1% hypoxia for 48h (**Figure 5B**). As expected, nuclear encoded genes involved in glycolytic metabolism such as pyruvate dehydrogenase kinase 1 (*PDK1*) or glyceraldehyde-3-phosphate dehydrogenase (*GAPDH*) were upregulated in hypoxia.

We quantified the mitochondria staining with MitoTracker in MCF7 and 786-0 cells exposed to normoxia or 0.1% hypoxia for 48h and no differences were observed (**Supplementary Figure 2A**).

Furthermore, we determined the expression of *POLRMT, TFAM* and *TFB1M* and some mitochondrial encoded genes in the parental 143B and Rho zero cells. *12S, ND3* and *ATP6* mitochondrial genes were absent in Rho Zero cells whereas *POLRMT, TFAM* and *TFB1M* were expressed as previously reported (32). However, hypoxia did not show any effect in the parental 143B cell line (**Supplementary Figure 2B**). This could be potentially related to the cytosolic thymidine kinase (TK1) deficiency of 143B cells (33) and the consequent downregulation in the expression of a subset of genes, some of which may protect mitochondria from stress (34). As the cytosolic and mitochondrial thymidine triphosphate pools are in rapid exchange and mainly produced by TK1 (35), it is possible that there is a more steady state of mtDNA replication in the TK1 deficient cells and hence mtdsRNA synthesis, with a stable source of nucleotides from the mitochondrial compartment produced by the mitochondrial thymidine kinase (TK2), which is not cell cycle regulated (36).

To support the hypothesis that hypoxia induced downregulation in the genes involved in mtDNA transcription would ultimately lead to less mtdsRNA formation, MCF7 cells were cultured with IMT1, a specific and non-competitive POLRMT inhibitor, and stained for dsRNA molecules. IMT1 dose-dependently reduced J2 staining, achieving the same levels as 0.1% hypoxia after treating the cells with 10μM (**Figure 6**).

Altogether, these data suggest that hypoxia leads to lower mtDNA transcription, without affecting the mitochondrial content, and thus lowers production of dsRNA available to trigger the type I IFN response.

Hypoxia Reduces Mitochondrial Ribosomal Protein Expression

It was also reported that hypoxia decreased protein expression of mitochondrial ribosomal proteins (MRPs) involved in mtRNA translation (37). We tested the expression of the mRNA coding for some of the MRPs under hypoxia in MCF7 cells and found that 16h of hypoxia significantly decreased their expression (**Figure 7A**), suggesting that less mtdsRNA in hypoxia could have a feedback mechanism on the expression of genes involved in mtRNA translation, as seen in bacteria (38). The same trend was observed in 786-0 WT and 786-0 KO cells, although it was not always statistically significant (**Figure 7B**), pointing to a HIF1α/HIF2α-independent mechanism.

mtRNA Is the Responsible for the *IFNβ* Promoter Induction

To assess the role of mtdsRNA in inducing the type I IFN pathway, MCF7 cells were cultured in normoxia or 0.1% hypoxia for 48h and their intact mitochondria were isolated. RNA from the mitochondrial and cytosolic fractions was extracted. Firstly, we confirmed that mitochondria were successfully enriched in the mitochondrial fraction by analysing the expression of several mitochondrial encoded genes in both fractions (**Figure 8A**). Then, these RNAs were transfected to HEK-293T P125 reporter cells to measure *IFNβ* promoter activation. The mitochondrial hypoxic and normoxic RNA extracts include mtRNA and also ssRNA. However, the *IFNβ* promoter assay only detects dsRNA. mtRNA induced *IFNβ* promoter stimulation, whereas the luciferase signal using cytosolic RNA was hardly detected. Importantly, hypoxic mtRNA caused significantly lower stimulation of *IFNβ* promoter (**Figure 8B**).

dsRNA-Enriched Fraction in Hypoxia Showed Lower mtRNA Content

To assess the composition of the dsRNA pool in hypoxia, dsRNA pull-down was performed using the J2 antibody in MCF7 cells exposed to normoxia or 0.1% hypoxia for 48h, and the resultant RNA was sequenced. Reads were normalised as transcript per million (TPM). Interestingly, the percentage of mitochondrial reads was significantly lower in hypoxia than in normoxia (**Figure 8C**), and 22 out of 37 mitochondrial encoded genes were significantly downregulated in hypoxia (**Supplementary Table 4**). Density plots in normoxia and hypoxia showed that the non-mitochondrial genes pulled-down by J2 antibody had few reads which probably correspond to background noise (red peak, **Figure 8D**).

Lower mtRNA in Hypoxia Is Not Due to Increase Mitophagy

To evaluate whether the downregulation of mtdsRNA in hypoxia was due to mitophagy, we knocked down one of the main genes involved in this process, *BNIP3* (BCL2 Interacting Protein 3) in MCF7 exposed to 0.1% hypoxia for 48h (siBNIP3 and control siRNA, siCON). In the knock-down cells, BNIP3 showed no induction in hypoxia, either at mRNA or protein level (**Figure 9A**). The expression of various ISGs (*DDX58*, *MX1*, *IFIT1*, *IFIT2*, *ADAR-p150* and *ISG15*) was tested. Hypoxia downregulated ISG expression (23), but no differences were found between siCON and siBNIP3 in hypoxia (**Figure 9B**), suggesting that hypoxic upregulation of BNIP3 does not interfere in the type I IFN signalling. This was further confirmed by the *IFNβ* promoter assay, in which hypoxia-induced inhibition on the *IFNβ* promoter activation was not recovered upon BNIP3 silencing (**Figure 9C**).

Live cell immunofluorescence was performed using mitochondrial and lysosomal markers in MCF7 cells cultured in normoxia or 0.1% hypoxia for 48h. As previously reported (29), mitochondria clearly exhibited morphological changes under low oxygen conditions and appeared more elongated and located closer to the nucleus (**Figure 9D**). However, no colocalization of the mitochondrial and lysosomal markers was

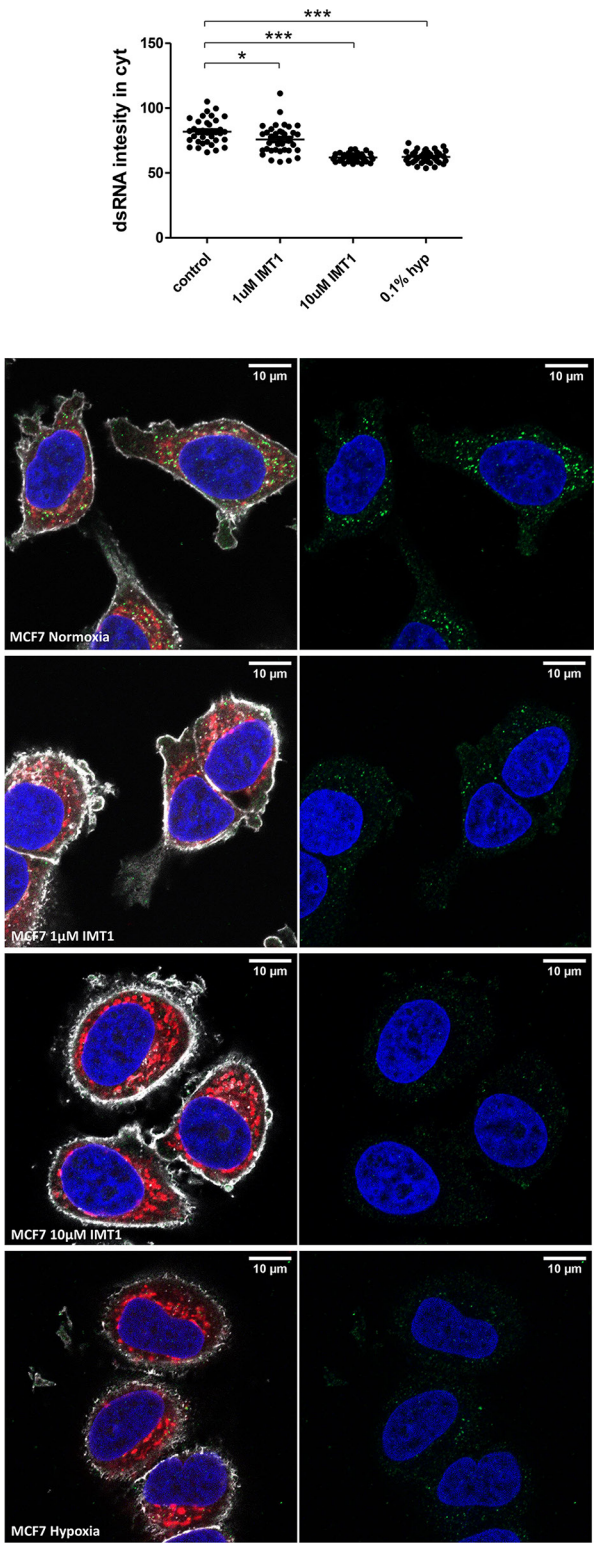

FIGURE 6 | IMT1 reduces dsRNA staining. dsRNA was stained using J2 antibody in MCF7 cells exposed to normoxia (n=36 cells), treated with 1µM IMT1 (n=36 cells), treated with 10µM IMT1 (n=36 cells) or exposed to 0.1% hypoxia (n=36 cells) for 48h from 3 independent replicates. Data is shown as mean ± SEM. *$p < 0.05$, ***$p < 0.001$. Green: J2 antibody staining, blue: DAPI, and red: MitoTracker staining. Scale bars correspond to 10µm.

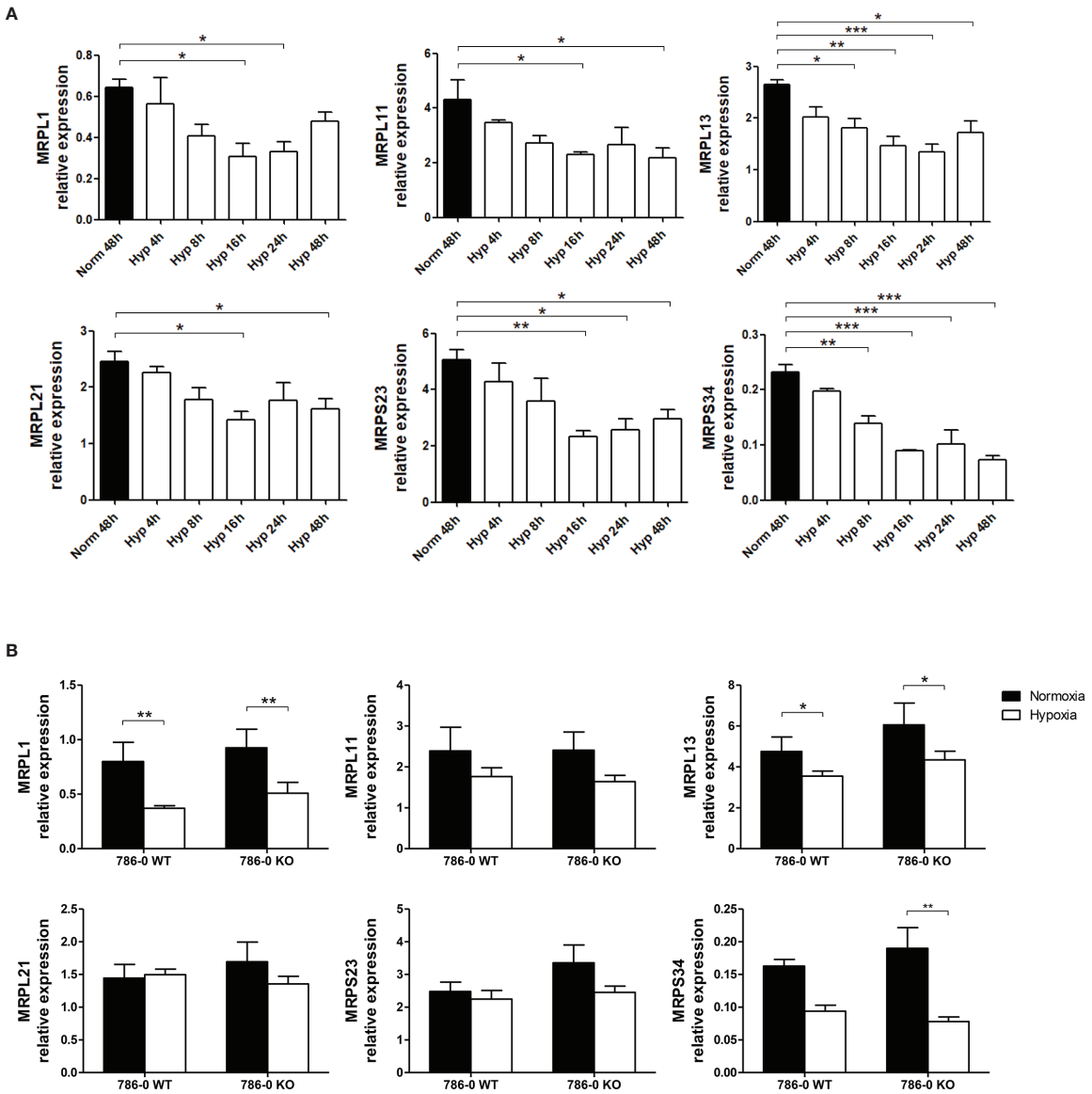

FIGURE 7 | Expression of mitochondrial ribosomal proteins (MRPs) is downregulated under hypoxia. **(A)** RNA expression of MRPs involved in mtRNA translation in MCF7 cells cultured in normoxia or 0.1% hypoxia for 4h, 8h, 16h, 24h and 48h was evaluated by qPCR (n=3). **(B)** MRPs mRNA expression in 786-0 WT and 786-0 KO cells cultured in normoxia or 0.1% hypoxia for 48h was also evaluated by qPCR (n=3). Number of replicates indicate biological replicates and data is shown as mean ± SEM. *p < 0.05, **p < 0.01, ***p < 0.001.

observed in normoxia or hypoxia, suggesting that mitophagy is not increased in hypoxia and does not decrease mtdsRNA.

Effect of Mitochondria-Targeting Drugs in dsRNA Levels

Next, the ability of different drugs targeting mitochondria to affect dsRNA levels was assessed in MCF7 cells. This was because drugs already approved or in preclinical trial may be detrimental to the normoxic response, or exacerbate the hypoxic suppression. Briefly, the drugs used were: chloramphenicol which inhibits mitochondrial protein synthesis *via* binding to the 50S subunit of the 70S mitochondrial ribosomes; ABT-737 induces cell apoptosis by inhibiting the anti-apoptotic molecule BCL2, as well as mitophagy; G-TPP accumulates in the mitochondria of tumour cells and by inhibiting the heat shock protein 90 (Hsp90) promotes cell apoptosis; mubritinib and metformin decrease mitochondrial respiration by inhibiting ETC complex I; and the Vps34 inhibitor SAR405 alters vesicle trafficking and inhibits autophagy by blocking autophagosome formation.

Mubritinib and G-TPP treatment decreased *IFNβ* promoter activation under normoxia by 4- and 2-fold, respectively (**Supplementary Figure 3**). Hypoxia did not further inhibit *IFNβ* promoter activity in MCF7 cells treated with these two drugs.

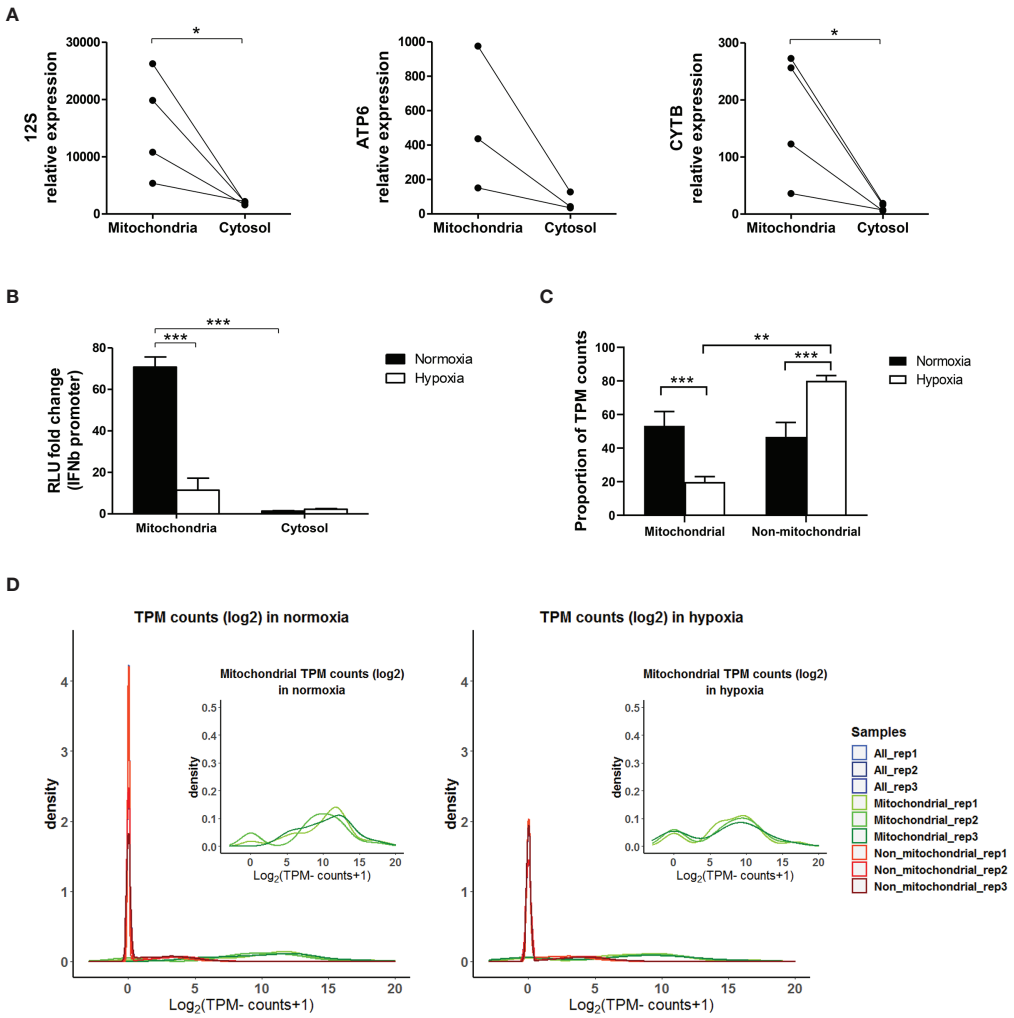

FIGURE 8 | Mitochondrial RNA is responsible for *IFNβ* promoter activation. **(A)** MCF7 cells cultured in normoxia for 48h were fractionated. RNA expression of mitochondrial encoded genes (*12S, ATP6, CYTB*) in mitochondrial and cytosolic fractions is shown by qPCR (n=3 or 4). **(B)** MCF7 cells cultured in normoxia or 0.1% hypoxia for 48h were fractionated and RNA from the mitochondria and cytosolic fractions was used to activate the *IFNβ* promoter (n=3; RLU, relative light units). **(C)** dsRNA pull down experiment using J2 antibody in MCF7 cells exposed to normoxia or 0.1% hypoxia for 48h was performed. Bar graph shows proportion of transcripts per million (TPM) mitochondrial and non-mitochondrial reads (n=3). **(D)** Density plots show mitochondrial (green), non-mitochondrial (red) and all reads (blue) in each replicate (rep) obtained from the dsRNA pull-down experiment in **(C)** (n=3). Number of replicates indicate biological replicates and data is shown as mean ± SEM. *$p < 0.05$, **$p < 0.01$, ***$p < 0.001$.

Tissue Distribution of Immunostimulatory RNA

Total RNA samples from different human tissues were obtained to assess their effects in the *IFNβ* promoter reporter assay. RNA from some tissues including brain, heart, kidney and testis strongly induced the *IFNβ* promoter reporter (**Figure 10A**). In contrast, RNA from other tissues, including skeletal muscle and pancreas, had little effect. ISG expression was also determined in RNA samples from some tissues. *MX1, IFIT1* and *IFNB1* exhibited much higher expression in testis and brain than in skeletal muscle (**Figure 10B**), confirming the results from the *IFNβ* promoter assay.

DISCUSSION

In this paper we have shown that hypoxia caused less formation of mtdsRNA in different cancer and normal cell lines leading to lower activation of *IFNβ* promoter. This repressive effect was HIF1α/2α-independent as hypoxia led to downregulation of mitochondrial gene expression in 786-0 HIF2α-KO cells, as in most other cell lines. However, 786-0 WT cells did not show lower mitochondrial gene expression in hypoxia. Those cells express only HIF2α, which enhances c-Myc transcriptional activity (39) and c-Myc increases the expression of POLRMT, thus increasing mtDNA transcription (40). Possibly this could compensate for the effect of hypoxia, and other transcription factors such as c-Jun and

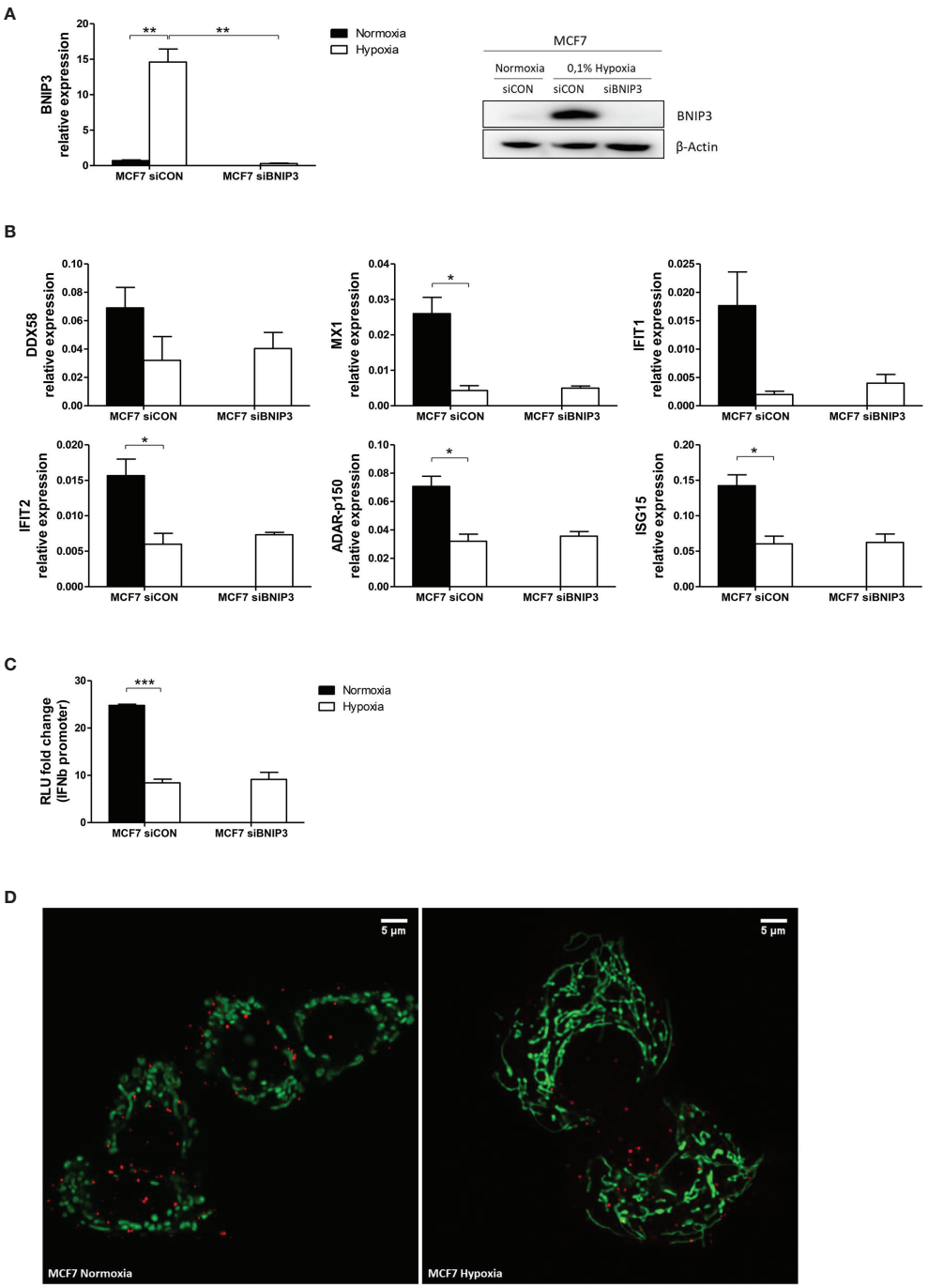

FIGURE 9 | Mitophagy is not involved in mtdsRNA reduction under hypoxia. **(A)** Silencing of BNIP3 was confirmed by qPCR (left panel) and western blot (right panel) in siBNIP3 MCF7 cells in hypoxia vs control (siCON) (n=3). **(B)** RNA expression of IFN-induced genes (ISGs) in siBNIP3 MCF7 cells vs siCON was performed by qPCR (n=3). **(C)** RNA from a) was used to evaluate *IFNβ* promoter activation after BNIP3 silencing (n=3; RLU, relative light units). **(D)** Representative image showing lack of colocalization between the mitochondrial (green) and lysosomal (red) markers in MCF7 cells exposed to normoxia or 0.1% hypoxia for 48h (n=3). Number of replicates indicate biological replicates and data is shown as mean ± SEM. *p < 0.05, **p < 0.01, ***p < 0.001. Scale bars correspond to 5µm.

NF-κB are noted to have a mitochondrial localisation and can be regulated in hypoxia in a HIF-independent manner (41).

Endogenous mtRNA, and specifically mtdsRNA, was responsible for triggering the *IFNβ* promoter activation *via* the MDA5/MAVS and not RIG-I/MAVS sensing pathway and the mechanism of reduction in hypoxia was investigated. It was recently reported that 99% of endogenous dsRNA was produced as a consequence of mtDNA transcription, and inhibition of the

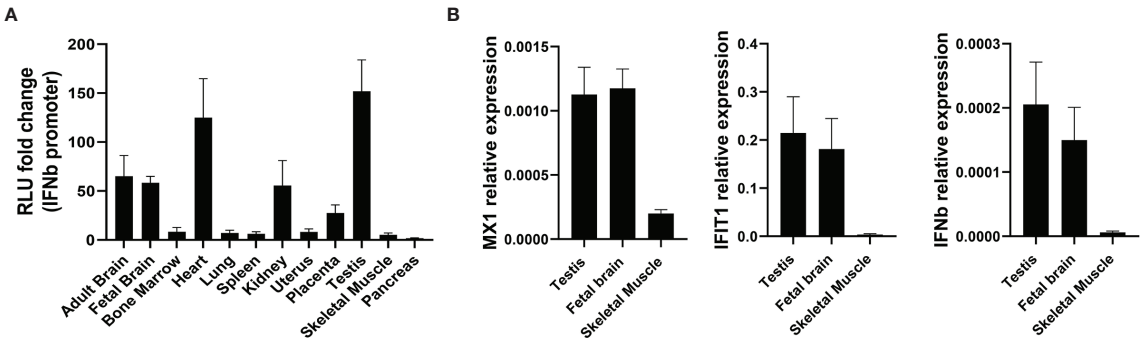

FIGURE 10 | The level of type I IFN pathway activation is tissue-dependent. **(A)** The *IFNβ* promoter reporter assay was used to assess the immunostimulatory properties of RNA samples from different tissues (n=3). **(B)** qPCR showing expression of *MX1, IFIT1* and *IFNβ* in different tissues from **(A)** (n=3). Number of replicates indicate biological replicates and data is shown as mean ± SEM.

mtdsRNA degrading enzyme PNPT1 increased type I IFN signalling (22). However, hypoxia did not affect the expression of SUV3 or PNPT1, thus suggesting that lower mtdsRNA presence in hypoxia could be a consequence of lower mitochondrial transcription under low oxygen conditions rather than higher degradation. Moreover, treating the cells with IMT1, a specific POLRMT inhibitor, decreased dsRNA levels as much as hypoxia, supporting that under hypoxia mtdsRNA levels were reduced due to lower mtDNA transcription.

dsRNA pull-down experiments showed that most of the reads corresponded to the mitochondrial chromosome. However, the percentage of mitochondrial reads was significantly lower in hypoxia and the expression of mitochondrial encoded genes was significantly downregulated. Supporting this hypothesis, we found decreased expression of mitochondrial encoded genes and nuclear encoded genes involved in mitochondrial transcription and translation when cells were cultured for only 4h under hypoxia, and it became significant at 16h. Moreover, dsRNA staining was also significantly lower at 16h under hypoxia. Other works reported a nuclear formation and accumulation of dsRNA when DICER was knocked down, but in that case dsRNAs were restricted to the nucleus, and they consisted of Satellite, rRNA and tRNA DNA sequences while long or short interspersed sequence (LINES and SINES) and long terminal repeat (LTR) elements were underrepresented (42). It was also reported in MEFs that *Trp53* deletion led to an increase on dsRNA, mainly originated from mitochondria, that triggered the type I IFN signalling pathway through MDA5 and to a lower extent RIG-I (43). They also showed that higher dsRNA content, in their case, was linked to overexpression of *OAS3* which activates *Rnase L* in order to degrade dsRNA into ssRNA. Interestingly, *OAS3* is significantly downregulated in hypoxia, together with *OAS2* and *OASL* (**Supplementary Table 5**), suggesting that lower endogenous dsRNA production in hypoxia would not require activation of a dsRNA degrading system.

Supporting our hypothesis of lower dsRNA production due to a decrease in mitochondrial transcription, when cells were treated with ethidium bromide to inhibit mitochondrial transcription without affecting nuclear transcription, a decreased in dsRNA formation and lower activation of the type I IFN signalling was observed (43). Moreover, recent data showed that PKR, which is another dsRNA sensing protein, binds preferentially to mtdsRNA over other sources of dsRNA (such as SINEs) and it is located both in the cytoplasm and mitochondria (3). We have shown that *PKR* levels are downregulated in hypoxia in a time dependent manner, as previously described for the dsRNA sensors RIG-I and MDA5 (23). Furthermore, our immunofluorescence data shows that PKR not only locates in the cytosol and mitochondria, but also in the nucleus, as previously reported (44), and that this nuclear localization is enhanced under hypoxia. Although it is unknown how PKR moves in and out of mitochondria, it is clear that it is not exclusively a mitochondrial protein (3). Interestingly, PKR is able to independently induce MAVS and trigger the type I IFN signalling, although the same paper also reported that PKR can cooperate with MDA5, but not with RIG-I, to induce IRF3 nuclear translocation (45). However, PKR is not able to independently induce *IFNβ* promoter as **Figure 1A** shows that MDA5 knockout cells completely abolished the activation.

These data suggest that PKR would be able to trigger the IFN response when enough mtdsRNA is produced and it could cooperate with MDA5 when the mitochondrial membrane is damaged and mtdsRNA leaked to the cytoplasm. Under hypoxia however, apart from lower PKR levels overall, PKR preferentially located in the nucleus where it interacts with noncoding nuclear RNAs (3). The release of dsRNA into the cytoplasm is additionally clearly a critical pathway for it to signal and the reduction in hypoxia will also decrease the amount that can be released by other stimuli used in therapy. During apoptosis, mitochondrial outer membrane permeabilization (MOMP) occurs, followed by caspase activation and a non-inflammatory cell death. However, cells usually die following MOMP even in the absence of caspase activation, through an inflammatory process initiated by mtDNA release to the cytoplasm and the consequent cGAS-STING pathway activation. This leads to pro-inflammatory cytokine production and an immune response that could initiate anti-tumour immunity (46). Moreover, some mitochondria within the cell can undergo MOMP in a stress-regulatory manner, which cannot induce enough caspase activation to trigger cell death. Instead, this leads to DNA damage, cellular transformation and tumorigenesis (47). We show that the

reservoir of dsRNA in mitochondria is reduced under hypoxia, hence, less to extract in the above experiments or signal when apoptosis or senescence occurs under hypoxic stress, being potentially beneficial for anti-tumour therapies.

Importantly, the capacity of the cell to detect dsRNA is dampened in hypoxia due to the downregulation of the sensing proteins, as our group has shown here and previously published (23). Hypoxia-induced mitophagy *via* BNIP3 was another possible explanation for decreased dsRNA formation (48, 49). However, our data showed that BNIP3 silencing did not revert the hypoxia-caused downregulation of several ISGs or *IFNβ* promoter activation. Also, live cell imaging of mitochondria and lysosomes supported this result, as no colocalization of mitochondrial and lysosomal markers was observed either in normoxia or hypoxia.

We investigated mitochondria-targeting drugs as potential regulators of dsRNA release, that may be detrimental in combination with immunotherapies. Low oxygen concentrations reduced the *IFNβ* promoter activation to the same extent as controls for most of the mitochondria-targeting drugs, and those inhibitors did not affect normoxic levels. Metformin, a complex I inhibitor, did not affect *IFNβ* promoter activation. In contrast, mubritinib [a much more potent inhibitor] and G-TPP caused a downregulation that reached hypoxic levels, with no further effect of hypoxia. G-TPP specifically inhibits the mitochondrial protein-folding chaperone Hsp90, generating unfolding protein stress in the mitochondria (50) which could decrease gene transcription. The similarity of reduction by these 2 inhibitors to that induced by hypoxia, and lack of further suppression, suggests these pathways could overlap, e.g. by inhibiting RNA synthesis.

Basal levels of dsRNA in different tissues without hypoxic stress was assessed using human total RNA, assuming that the assay measured only dsRNA. RNA from testis, brain, heart and kidney were strong activators of *IFNβ* promoter, and these tissues also showed higher expression of type I IFN genes (*MX1, IFIT1* and *IFNB1*). Mitochondrial mass is well correlated with citrate synthase and cytochrome oxidase activity, mtDNA copy number and mitochondrial gene expression, and all these parameters are greater in tissues with higher bioenergetics and metabolic demands such as heart (51). Although skeletal muscle RNA hardly triggered *IFNβ* promoter activation whereas heart RNA was far more effective, this could be explained by low basal activity of mitochondria in resting striated muscle. Additionally, higher oxygen concentrations in tissues such as brain, heart and kidney could stimulate higher turnover (52). Interestingly, some tumour types such as bladder, breast, esophageal, head and neck, kidney and liver showed significantly lower mtDNA content than paired adjacent normal tissue, and this was associated with lower patient survival (53). Expression could be even lower in hypoxic areas having impact in anticancer therapies that rely on a functional type I IFN signalling. Moreover, it has recently been shown that hypoxic monocytes are unable to produce type I IFNs (54), potentially reducing the antitumor response.

To sum up, we have shown that hypoxia caused significantly lower mtdsRNA production, probably due to a decrease in mitochondrial transcription rather than increased degradation, thus leading to lower activation of *IFNβ* promoter, and consequently to lower type I IFN response that could contribute to the immunosuppression observed in hypoxic environments and to chemotherapy and radiotherapy resistance.

DATA AVAILABILITY STATEMENT

The datasets presented in this study can be found in online repositories. The names of the repository/repositories and accession number(s) can be found below: https://www.ncbi.nlm.nih.gov/, GSE153557.

ETHICS STATEMENT

Ethical review and approval was not required for the study on human participants in accordance with the local legislation and institutional requirements. Written informed consent for participation was not required for this study in accordance with the national legislation and the institutional requirements.

AUTHOR CONTRIBUTIONS

EA, AM, JR, and AH designed the experiments, analysed the data and wrote the manuscript. EA and AM performed the experiments. AD developed the *IFNβ* promoter assay and performed this assay for **Figure 1A** and **Figure 10A**. US and DW developed the ImageJ macro to quantify J2 immunofluorescence. NP performed all RNA-seq and J2-IP analysis. JN reviewed the manuscript. All authors contributed to the article and approved the submitted version.

FUNDING

This research was supported by funding from Cancer Research UK (AH), Breast Cancer Research Foundation (AH), and Breast Cancer Now [AH, AM, (2015MayPR479)].

ACKNOWLEDGMENTS

We thank Dr Karl Morten (University of Oxford, UK) for the 143B and Rho Zero cells, Dr Charles Lawrie (Biodonostia Instituto de Investigación Sanitaria, Spain) for the 786-0 WT and HIF2α-KO cells, and Dr Christian Frezza (University of Cambridge, UK) for the mTUNE cells.

SUPPLEMENTARY MATERIAL

The Supplementary Material for this article can be found online at: https://www.frontiersin.org/articles/10.3389/fonc.2021.779739/full#supplementary-material

REFERENCES

1. Rehwinkel J, Gack MU. RIG-I-Like Receptors: Their Regulation and Roles in RNA Sensing. *Nat Rev Immunol* (2020) 20(9):537–51. doi: 10.1038/s41577-020-0288-3
2. McNab F, Mayer-Barber K, Sher A, Wack A, O'Garra A. Type I Interferons in Infectious Disease. *Nat Rev Immunol* (2015) 15(2):87–103. doi: 10.1038/nri3787
3. Kim Y, Park J, Kim S, Kim M, Kang MG, Kwak C, et al. PKR Senses Nuclear and Mitochondrial Signals by Interacting With Endogenous Double-Stranded RNAs. *Mol Cell* (2018) 71(6):1051–63.e6. doi: 10.1016/j.molcel.2018.07.029
4. Honda K, Takaoka A, Taniguchi T. Type I Interferon [Corrected] Gene Induction by the Interferon Regulatory Factor Family of Transcription Factors. *Immunity* (2006) 25(3):349–60. doi: 10.1016/j.immuni.2006.08.009
5. Stark GR, Darnell JEJr. The JAK-STAT Pathway at Twenty. *Immunity* (2012) 36(4):503–14. doi: 10.1016/j.immuni.2012.03.013
6. Chukwurah E, Farabaugh KT, Guan B-J, Ramakrishnan P, Hatzoglou M. A Tale of Two Proteins: PACT and PKR and Their Roles in Inflammation. *FEBS J* (2021) 288(22):6365–91. doi: 10.1111/febs.15691
7. Gil J, Garcia MA, Gomez-Puertas P, Guerra S, Rullas J, Nakano H, et al. TRAF Family Proteins Link PKR With NF-Kappa B Activation. *Mol Cell Biol* (2004) 24(10):4502–12. doi: 10.1128/MCB.24.10.4502-4512.2004
8. Zitvogel L, Galluzzi L, Kepp O, Smyth MJ, Kroemer G. Type I Interferons in Anticancer Immunity. *Nat Rev Immunol* (2015) 15(7):405–14. doi: 10.1038/nri3845
9. Budhwani M, Mazzieri R, Dolcetti R. Plasticity of Type I Interferon-Mediated Responses in Cancer Therapy: From Anti-Tumor Immunity to Resistance. *Front Oncol* (2018) 8:322. doi: 10.3389/fonc.2018.00322
10. Noman MZ, Hasmim M, Messai Y, Terry S, Kieda C, Janji B, et al. Hypoxia: A Key Player in Antitumor Immune Response. A Review in the Theme: Cellular Responses to Hypoxia. *Am J Physiol Cell Physiol* (2015) 309(9):C569–79. doi: 10.1152/ajpcell.00207.2015
11. Noman MZ, Messai Y, Carre T, Akalay I, Meron M, Janji B, et al. Microenvironmental Hypoxia Orchestrating the Cell Stroma Cross Talk, Tumor Progression and Antitumor Response. *Crit Rev Immunol* (2011) 31(5):357–77. doi: 10.1615/CritRevImmunol.v31.i5.10
12. Feder-Mengus C, Ghosh S, Weber WP, Wyler S, Zajac P, Terracciano L, et al. Multiple Mechanisms Underlie Defective Recognition of Melanoma Cells Cultured in Three-Dimensional Architectures by Antigen-Specific Cytotoxic T Lymphocytes. *Br J Cancer* (2007) 96(7):1072–82. doi: 10.1038/sj.bjc.6603664
13. Husain Z, Huang Y, Seth P, Sukhatme VP. Tumor-Derived Lactate Modifies Antitumor Immune Response: Effect on Myeloid-Derived Suppressor Cells and NK Cells. *J Immunol (Baltimore Md: 1950)* (2013) 191(3):1486–95. doi: 10.4049/jimmunol.1202702
14. Zhang W, Wang G, Xu ZG, Tu H, Hu F, Dai J, et al. Lactate Is a Natural Suppressor of RLR Signaling by Targeting MAVS. *Cell* (2019) 178(1):176–89 e15. doi: 10.1016/j.cell.2019.05.003
15. Andrews RM, Kubacka I, Chinnery PF, Lightowlers RN, Turnbull DM, Howell N. Reanalysis and Revision of the Cambridge Reference Sequence for Human Mitochondrial DNA. *Nat Genet* (1999) 23(2):147. doi: 10.1038/13779
16. Anderson S, Bankier AT, Barrell BG, de Bruijn MH, Coulson AR, Drouin J, et al. Sequence and Organization of the Human Mitochondrial Genome. *Nature* (1981) 290(5806):457–65. doi: 10.1038/290457a0
17. Pallen MJ. Time to Recognise That Mitochondria Are Bacteria? *Trends Microbiol* (2011) 19(2):58–64. doi: 10.1016/j.tim.2010.11.001
18. Zhang Q, Raoof M, Chen Y, Sumi Y, Sursal T, Junger W, et al. Circulating Mitochondrial DAMPs Cause Inflammatory Responses to Injury. *Nature* (2010) 464(7285):104–7. doi: 10.1038/nature08780
19. Zhou R, Yazdi AS, Menu P, Tschopp J. A Role for Mitochondria in NLRP3 Inflammasome Activation. *Nature* (2011) 475:122. doi: 10.1038/nature10156
20. Rongvaux A, Jackson R, Harman CC, Li T, West AP, de Zoete MR, et al. Apoptotic Caspases Prevent the Induction of Type I Interferons by Mitochondrial DNA. *Cell* (2014) 159(7):1563–77. doi: 10.1016/j.cell.2014.11.037
21. Krüger A, Oldenburg M, Chebrolu C, Beisser D, Kolter J, Sigmund AM, et al. Human TLR8 Senses UR/URR Motifs in Bacterial and Mitochondrial RNA. *EMBO Rep* (2015) 16(12):1656–63. doi: 10.15252/embr.201540861
22. Dhir A, Dhir S, Borowski LS, Jimenez L, Teitell M, Rotig A, et al. Mitochondrial Double-Stranded RNA Triggers Antiviral Signalling in Humans. *Nature* (2018) 560(7717):238–42. doi: 10.1038/s41586-018-0363-0
23. Miar A, Arnaiz E, Bridges E, Beedie S, Cribbs AP, Downes DJ, et al. Hypoxia Induces Transcriptional and Translational Downregulation of the Type I IFN Pathway in Multiple Cancer Cell Types. *Cancer Res* (2020) 80(23):5245–56. doi: 10.1158/0008-5472.CAN-19-2306
24. Gaude E, Schmidt C, Gammage PA, Dugourd A, Blacker T, Chew SP, et al. NADH Shuttling Couples Cytosolic Reductive Carboxylation of Glutamine With Glycolysis in Cells With Mitochondrial Dysfunction. *Mol Cell* (2018) 69(4):581–93.e7. doi: 10.1016/j.molcel.2018.01.034
25. Cochrane EJ, Hulit J, Lagasse FP, Lechertier T, Stevenson B, Tudor C, et al. Impact of Mitochondrial Targeting Antibiotics on Mitochondrial Function and Proliferation of Cancer Cells. *ACS Med Chem Lett* (2021) 12(4):579–84. doi: 10.1021/acsmedchemlett.0c00632
26. Hertzog J, Dias Junior AG, Rigby RE, Donald CL, Mayer A, Sezgin E, et al. Infection With a Brazilian Isolate of Zika Virus Generates RIG-I Stimulatory RNA and the Viral NS5 Protein Blocks Type I IFN Induction and Signaling. *Eur J Immunol* (2018) 48(7):1120–36. doi: 10.1002/eji.201847483
27. Burger K, Schlackow M, Potts M, Hester S, Mohammed S, Gullerova M. Nuclear Phosphorylated Dicer Processes Double-Stranded RNA in Response to DNA Damage. *J Cell Biol* (2017) 216(8):2373–89. doi: 10.1083/jcb.201612131
28. Eales KL, Hollinshead KE, Tennant DA. Hypoxia and Metabolic Adaptation of Cancer Cells. *Oncogenesis* (2016) 5:e190. doi: 10.1038/oncsis.2015.50
29. Chiche J, Rouleau M, Gounon P, Brahimi-Horn MC, Pouyssegur J, Mazure NM. Hypoxic Enlarged Mitochondria Protect Cancer Cells From Apoptotic Stimuli. *J Cell Physiol* (2010) 222(3):648–57. doi: 10.1002/jcp.21984
30. Thomas LW, Staples O, Turmaine M, Ashcroft M. CHCHD4 Regulates Intracellular Oxygenation and Perinuclear Distribution of Mitochondria. *Front Oncol* (2017) 7:71. doi: 10.3389/fonc.2017.00071
31. Calvo SE, Clauser KR, Mootha VK. MitoCarta2.0: An Updated Inventory of Mammalian Mitochondrial Proteins. *Nucleic Acids Res* (2016) 44(D1):D1251–7. doi: 10.1093/nar/gkv1003
32. Wilson WL, LeBelle MJ. Identification of an Imidazolinium Salt, the Major Product From Reaction of Benzathine With Iodine. *J Pharm Sci* (1979) 68(10):1322–3. doi: 10.1002/jps.2600681035
33. King MP, Attardi G. Isolation of Human Cell Lines Lacking Mitochondrial DNA. *Methods Enzymol* (1996) 264:304–13. doi: 10.1016/S0076-6879(96)64029-4
34. Malvi P, Janostiak R, Nagarajan A, Cai G, Wajapeyee N. Loss of Thymidine Kinase 1 Inhibits Lung Cancer Growth and Metastatic Attributes by Reducing GDF15 Expression. *PloS Genet* (2019) 15(10):e1008439–e. doi: 10.1371/journal.pgen.1008439
35. Pontarin G, Gallinaro L, Ferraro P, Reichard P, Bianchi V. Origins of Mitochondrial Thymidine Triphosphate: Dynamic Relations to Cytosolic Pools. *Proc Natl Acad Sci USA* (2003) 100(21):12159–64. doi: 10.1073/pnas.1635259100
36. King MP, Attardi G. Human Cells Lacking mtDNA: Repopulation With Exogenous Mitochondria by Complementation. *Sci (New York NY)* (1989) 246(4929):500–3. doi: 10.1126/science.2814477
37. Bousquet PA, Sandvik JA, Arntzen MO, Jeppesen Edin NF, Christoffersen S, Krengel U, et al. Hypoxia Strongly Affects Mitochondrial Ribosomal Proteins and Translocases, as Shown by Quantitative Proteomics of HeLa Cells. *Int J Proteomics* (2015) 2015:678527. doi: 10.1155/2015/678527
38. Ralston A. Simultaneous Gene Transcription and Translation in Bacteria. *Nat Educ* (2008) 1(4).
39. Gordan JD, Bertout JA, Hu CJ, Diehl JA, Simon MC. HIF-2alpha Promotes Hypoxic Cell Proliferation by Enhancing C-Myc Transcriptional Activity. *Cancer Cell* (2007) 11(4):335–47. doi: 10.1016/j.ccr.2007.02.006
40. Oran AR, Adams CM, Zhang XY, Gennaro VJ, Pfeiffer HK, Mellert HS, et al. Multi-Focal Control of Mitochondrial Gene Expression by Oncogenic MYC Provides Potential Therapeutic Targets in Cancer. *Oncotarget* (2016) 7(45):72395–414. doi: 10.18632/oncotarget.11718
41. Barshad G, Marom S, Cohen T, Mishmar D. Mitochondrial DNA Transcription and Its Regulation: An Evolutionary Perspective. *Trends Genet* (2018) 34(9):682–92. doi: 10.1016/j.tig.2018.05.009

42. White E, Schlackow M, Kamieniarz-Gdula K, Proudfoot NJ, Gullerova M. Human Nuclear Dicer Restricts the Deleterious Accumulation of Endogenous Double-Stranded RNA. *Nat Struct Mol Biol* (2014) 21(6):552–9. doi: 10.1038/nsmb.2827
43. Wiatrek DM, Candela ME, Sedmik J, Oppelt J, Keegan LP, O'Connell MA. Activation of Innate Immunity by Mitochondrial dsRNA in Mouse Cells Lacking P53 Protein. *RNA (New York NY)* (2019) 25(6):713–26. doi: 10.1261/rna.069625.118
44. Jeffrey IW, Kadereit S, Meurs EF, Metzger T, Bachmann M, Schwemmle M, et al. Nuclear Localization of the Interferon-Inducible Protein Kinase PKR in Human Cells and Transfected Mouse Cells. *Exp Cell Res* (1995) 218(1):17–27. doi: 10.1006/excr.1995.1126
45. Pham AM, Santa Maria FG, Lahiri T, Friedman E, Marie IJ, Levy DE. PKR Transduces MDA5-Dependent Signals for Type I IFN Induction. *PloS Pathog* (2016) 12(3):e1005489. doi: 10.1371/journal.ppat.1005489
46. Giampazolias E, Zunino B, Dhayade S, Bock F, Cloix C, Cao K, et al. Mitochondrial Permeabilization Engages NF-κb-Dependent Anti-Tumour Activity Under Caspase Deficiency. *Nat Cell Biol* (2017) 19(9):1116–29. doi: 10.1038/ncb3596
47. Ichim G, Lopez J, Ahmed SU, Muthalagu N, Giampazolias E, Delgado ME, et al. Limited Mitochondrial Permeabilization Causes DNA Damage and Genomic Instability in the Absence of Cell Death. *Mol Cell* (2015) 57(5):860–72. doi: 10.1016/j.molcel.2015.01.018
48. Sowter HM, Ratcliffe PJ, Watson P, Greenberg AH, Harris AL. HIF-1-Dependent Regulation of Hypoxic Induction of the Cell Death Factors BNIP3 and NIX in Human Tumors. *Cancer Res* (2001) 61(18):6669–73.
49. Zhang H, Bosch-Marce M, Shimoda LA, Tan YS, Baek JH, Wesley JB, et al. Mitochondrial Autophagy Is an HIF-1-Dependent Adaptive Metabolic Response to Hypoxia. *J Biol Chem* (2008) 283(16):10892–903. doi: 10.1074/jbc.M800102200
50. Kang BH, Plescia J, Song HY, Meli M, Colombo G, Beebe K, et al. Combinatorial Drug Design Targeting Multiple Cancer Signaling Networks Controlled by Mitochondrial Hsp90. *J Clin Invest* (2009) 119(3):454–64. doi: 10.1172/JCI37613
51. D'Erchia AM, Atlante A, Gadaleta G, Pavesi G, Chiara M, De Virgilio C, et al. Tissue-Specific mtDNA Abundance From Exome Data and Its Correlation With Mitochondrial Transcription, Mass and Respiratory Activity. *Mitochondrion* (2015) 20:13–21. doi: 10.1016/j.mito.2014.10.005
52. Krysko DV, Agostinis P, Krysko O, Garg AD, Bachert C, Lambrecht BN, et al. Emerging Role of Damage-Associated Molecular Patterns Derived From Mitochondria in Inflammation. *Trends Immunol* (2011) 32(4):157–64. doi: 10.1016/j.it.2011.01.005
53. Reznik E, Miller ML, Senbabaoglu Y, Riaz N, Sarungbam J, Tickoo SK, et al. Mitochondrial DNA Copy Number Variation Across Human Cancers. *eLife* (2016) 5. doi: 10.7554/eLife.10769
54. Peng T, Du SY, Son M, Diamond B. HIF-1α Is a Negative Regulator of Interferon Regulatory Factors: Implications for Interferon Production by Hypoxic Monocytes. *Proc Natl Acad Sci USA* (2021) 118(26). doi: 10.1073/pnas.2106017118

Conflict of Interest: The authors declare that the research was conducted in the absence of any commercial or financial relationships that could be construed as a potential conflict of interest.

Publisher's Note: All claims expressed in this article are solely those of the authors and do not necessarily represent those of their affiliated organizations, or those of the publisher, the editors and the reviewers. Any product that may be evaluated in this article, or claim that may be made by its manufacturer, is not guaranteed or endorsed by the publisher.